Effect of microstructure on the plasma surface treatment of carbon fibres

Corujeira Gallo, Santiago; Dong, Hanshan

DOI:
10.1177/0021998316684935

Document Version
Peer reviewed version

Citation for published version (Harvard):
Corujeira Gallo, S & Dong, H 2016, 'Effect of microstructure on the plasma surface treatment of carbon fibres', *Journal of Composite Materials*. https://doi.org/10.1177/0021998316684935

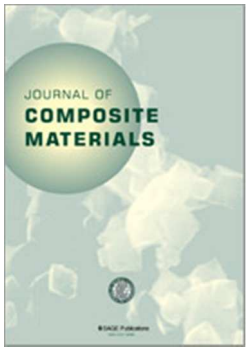

Effect of microstructure on the plasma surface treatment of carbon fibres

Journal:	*Journal of Composite Materials*
Manuscript ID	JCM-16-0726.R2
Manuscript Type:	Review
Date Submitted by the Author:	n/a
Complete List of Authors:	Corujeira Gallo, Santiago; University of Birmingham, School of Metallurgy and Materials Dong, Hanshan; University of Birmingham, School of Metallurgy and Materials
Keywords:	carbon fibres, polymer-matrix composites, fibre/matrix bond, surface treatments, plasma
Abstract:	Carbon fibres are leading reinforcements in composite materials because of their outstanding mechanical and physical properties. However, the graphitic surface of these fibres is relatively inert, and the weak interaction between the carbon fibres and the polymeric matrix has negative consequences for the mechanical properties of composite materials. Surface treatments have been used to increase the surface roughness, remove contaminants or weakly bonded layers, and to alter the surface chemistry and wettability of the fibres. In this article, the authors review the effect of the microstructure on the response of the carbon fibres to the surface treatments. The observations from conventional carbon fibres and functionalisation techniques are extrapolated to plasma surface treatments and to novel carbon fibres produced from bio-precursors.

Article type: Review

Corresponding author information: Santiago Corujeira-Gallo

School of Metallurgy and Materials

University of Birmingham

Edgbaston, Birmingham

B15 2TT, United Kingdom

E-mail: corujeis@bham.ac.uk

Telephone: +44 (0) 121 414 5163

Article title: Effect of microstructure on the plasma surface treatment of carbon fibres

Authors: Santiago Corujeira-Gallo

School of Metallurgy and Materials, University of Birmingham, UK

Hanshan Dong

School of Metallurgy and Materials, University of Birmingham, UK

Abstract

Carbon fibres are leading reinforcements in composite materials because of their outstanding mechanical and physical properties. However, the graphitic surface of these fibres is relatively inert, and the weak interaction between the carbon fibres and the polymeric matrix has negative consequences for the mechanical properties of composite materials. Surface treatments have been used to increase the surface roughness, remove contaminants or weakly bonded layers, and to alter the surface chemistry and wettability of the fibres. In this article, the authors review the effect of the microstructure on the response of the carbon fibres to the surface treatments. The observations from conventional carbon fibres and functionalisation techniques are extrapolated to plasma surface treatments and to novel carbon fibres produced from bio-precursors.

Effect of microstructure on the plasma surface treatment of carbon fibres

Santiago Corujeira-Gallo and Hanshan Dong

University of Birmingham, School of Metallurgy and Materials

Edgbaston, Birmingham, B15 2TT, United Kingdom

Corresponding author: corujeis@bham.ac.uk

Telephone: +44 (0) 121 414 5163

Abstract

Carbon fibres are leading reinforcements in composite materials because of their outstanding mechanical and physical properties. However, the graphitic surface of these fibres is relatively inert, and the weak interaction between the carbon fibres and the polymeric matrix has negative consequences for the mechanical properties of composite materials. Surface treatments have been used to increase the surface roughness, remove contaminants or weakly bonded layers, and to alter the surface chemistry and wettability of the fibres. In this article, the authors review the effect of the microstructure on the response of the carbon fibres to the surface treatments. The observations from conventional carbon fibres and functionalisation techniques are extrapolated to plasma surface treatments and to novel carbon fibres produced from bio-precursors.

Keywords: carbon fibres, polymer-matrix composites, Fibre/matrix bond, surface treatments.

1. Introduction

The interface between the reinforcing fibres and the polymeric matrix is of utmost importance for the mechanical properties of composite materials [1]. Therefore, a thorough understanding of the interaction mechanisms between carbon fibres (CFs) and polymers is

essential to design and tailor the properties of composites. High interfacial shear strength (IFSS) between the CFs and the polymeric matrix tends to produce composites with high ultimate strength, which are appropriate for structural applications. On the other hand, a low IFSS tends to result in tough composites with application in energy-absorbing components. Consequently, the optimum IFSS depends on the specific demands of each application, and the ability to modify it is very important.

The IFSS between the reinforcing fibres and the polymer is usually attributed to chemical, physical and mechanical interactions [1, 2]. For a given polymer, the IFSS is determined by the microstructure of the fibres and the presence of defects on their surface, their roughness and surface morphology, their surface area, the chemical groups attached to the surface, the surface free energy of the fibres and their wettability by the polymer. Even though the microstructure of CFs varies with the nature of the precursors and with the processing conditions [2], a high density of graphitic basal planes is typically observed on their surface. These fully bonded basal crystals are chemically inert and exhibit poor wettability and low interaction with polymers.

Therefore, surface treatments are normally applied to CFs, in order to improve their interaction with the polymeric matrix. These treatments aim to remove contaminants from the surface of the fibres, eliminate weakly bonded carbon planes, increase the roughness and/or attach chemically active groups to their surface [1]. Over the years, many different technologies have been used to modify the surface properties of CFs, and these include: wet chemical methods with strong acids [3] or basic solutions [4], wet electrochemical methods [5], chemical or physical activation by oxidation in the gas phase [6], application of thin coatings [7] or nanostructures on the surface [8], plasma treatments with oxidative or non-oxidative gases (both atmospheric [9] and low-pressure [10]), or a combination of several of these treatments [11].

Several authors have noted a different response of carbon fibres to the surface treatments, depending on their microstructure [12-15]. Their observations take a new dimension based on the recent interest on carbon fibres developed from bio-precursors [16, 17]. This article offers a critical review of seminal papers and recent literature regarding the microstructure of CFs, its effect on the surface treatment and, ultimately, the nature of their bond with polymers in composite materials. The discussions are enriched with observations from several technologies, although particular attention is given to plasma treatments, with focus on non-polymerising low-pressure plasmas. The authors provide a complementary view to the excellent review papers published in past years [2, 18-20].

2. Microstructure of carbon fibres

The manufacturing process of CFs typically involves: extruding or spinning a polymeric precursor to form fibres, their stabilisation at moderate temperatures and their subsequent carbonisation or graphitisation at high temperature. To this end, it is well known that the microstructure of CFs is a function of the precursor polymer and of the processing conditions.

2.a. Precursor fibres

Polyacrylonitrile (PAN) and mesophase pitch (MPP) are two of the most common precursors used in the fabrication of carbon fibres (CFs). Some researchers have studied the structure of the precursor fibres, and the relationship between the microstructure of the parent PAN or MPP fibre and the resulting CF. Bai et al. [21] conducted high resolution transmission electron microscopy (HR-TEM) studies on PAN precursor fibres, spun from a solution of 20% copolymer of acrylonitrile and itaconic acid after polymerisation in dimethylsulfoxide using 2,20-azobisisobutyronitrile (AIBN) as initiator. The solution was extruded through a spinneret and drawn in a coagulation bath, with a total drawing ratio of 1200%.

A spherical morphology was observed in the transverse cross section of these precursor PAN fibres [21]. The spheres had a multilayered (onion-like) fullerene structure and were interlinked, despite having some interstices among them. Their formation mechanism is unclear, although a theory based on dipolar nitrile group interactions was proposed. In addition to the spheres, nanosized crystallites were found distributed in an amorphous matrix. The lattice fringes observed under HRTEM were compared with the crystalline carbon (or graphite) and had various orientations in different crystallites. The interplanar spacing's of the (010) and (210) planes of PAN were 0.346 nm and 0.527 nm, respectively (Figure 1a).

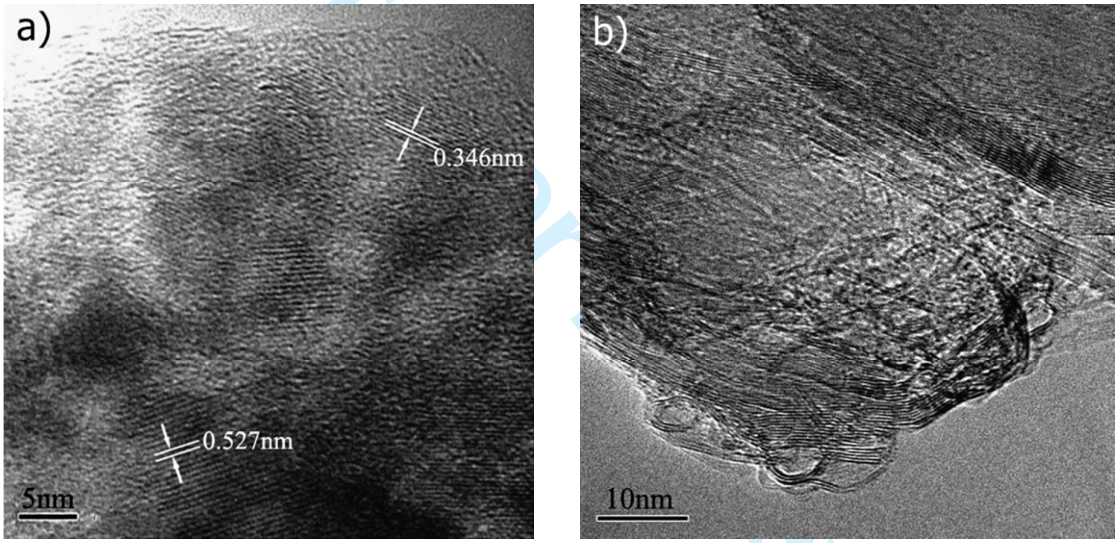

Figure 1: HR-TEM micrographs of PAN fibres: a) transverse and b) longitudinal cross-sections [21].

The microstructure observed in the longitudinal section of the same PAN fibres was considerably different, and consisted of ribbon like structures with clear lattice fringes [21]. The ribbons were entangled and formed a networked morphology, but exhibited a preferential orientation along the fibre axis (Figure 1b). This preferential orientation forms during the stretching of the PAN fibres and enhances their tensile strength. However, the strain

distribution during the stretching of the fibres is not uniform, and this results in a complex microstructure. The authors also found elongated pores, which are believed to form by solvent diffusion in the coagulation bath, and subsequently elongated during the stretching of the fibres.

2.b. Stabilised fibres

The stabilisation of precursor fibres is typically conducted between 220°C and 280°C in air. It is an exothermic process that involves the dehydrogenation, oxidation and cross linking of the PAN precursor fibre. The stabilisation is believed to affect the microstructure of the precursor fibres and the mechanical properties of the resulting CF. Ge et al. [22] studied the microstructure of PAN fibres stabilised in air at temperatures between 190°C and 275°C, and under a 5% stretching ratio. The stabilisation time in each temperature zone was 6 minutes, and the total stabilisation time was approximately 60 minutes.

The stabilised PAN fibres had a skin-core microstructure and a concentric multilayer structure in their core [22]. The skin was compact and exhibited a strong texture, while the core had a disordered microstructure. The different microstructures were associated with different oxygen contents in each layer. This was attributed to the cross-linking and aromatic structures formed through reactions with oxygen during stabilisation.

The HR-TEM observations, conducted on the transverse cross section of stabilised fibres, revealed a spherical morphology, with a multilayered (onion-like) fullerene structure, similar to the one described previously [22]. The spheres decreased in size, and exhibited an amorphous structure in their exterior and nanosized crystallites in their interior, with various orientations. These crystallite structures were found to be analogous to the ones observed in CFs. Therefore, it was suggested that there exists a direct correlation between the orientation and arrangement of molecule chains in the precursor fibres and in the stabilised fibres.

2.c. Carbon fibres

Carbon fibres are produced by pyrolysis of the stabilised precursors in inert atmospheres [16]. The pyrolysis process is conducted under tension to retain the atomic alignment [23]. In this process, the volatile components are removed, leaving CFs with a carbon content of over 98%. The carbon yield of the precursors has a significant impact on the final microstructure, the content of porosity and the mechanical properties of the carbon fibres [24].

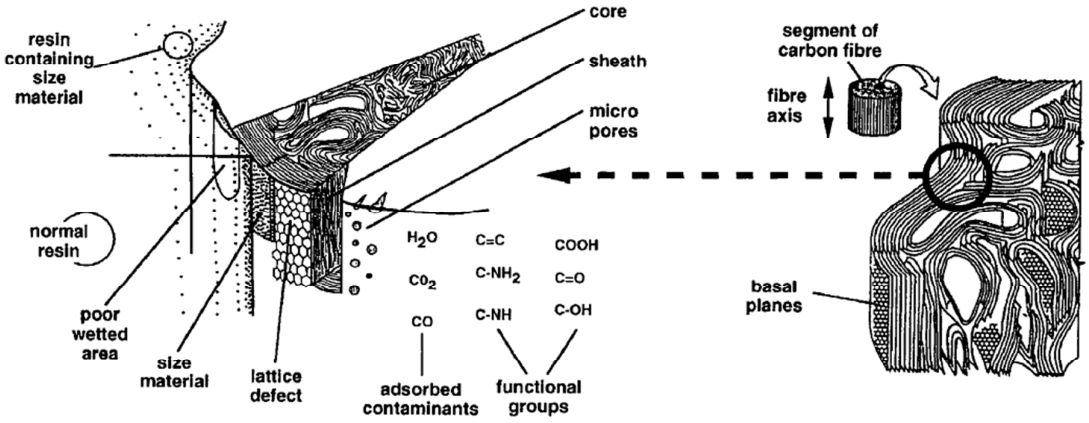

Figure 2: Schematic diagram of the surface structure of ex-PAN carbon fibres [25, 26] cited in [1]

The microstructure of CFs is often described as turbostratic, as illustrated in Figure 2 [25, 26] cited in [1]. This structure consists of parallel layers of aromatic planes, some of which form crystallites similar to the graphite structure but arranged at random angular orientations [27-29]. In addition, CFs exhibit structural heterogeneity in terms of skin-core structure. The outer skin has a highly oriented turbostratic structure, whereas the core shows a lower degree of alignment with respect to the fibre axis. The elastic modulus of CFs increases with the degree of orientation of the layer planes along the fibre axis. As a result, the elastic modulus of the skin is higher than the core. Kowbel et al. [30] linked this structural heterogeneity with the

development of residual stresses upon cooling from the processing temperature, leaving the skin under compression and the core under tension.

In a thorough review article [31], Edie summarised the differences between ex-PAN and ex-MPP carbon fibres, and their respective processing conditions, microstructures and properties. Ex-PAN CFs have a discontinuous and less ordered fibrillar structure, with extensively folded and interlinked turbostratic layers of carbon and interlayer spacing considerably larger than those of graphite. As a result, ex-PAN CFs exhibit higher strength but lower elastic modulus than ex-MPP CFs. Edie also found that the tensile strength of ex-PAN CFs increased with the carbonisation temperatures up to 1600°C, but dropped markedly beyond this point as a result of the evolution of nitrogen and the formation of porosity and defects in the microstructure.

Qin et al. [32] studied the microstructure and the mechanical properties of ex-PAN and ex-MPP CFs, graphitised at temperatures between 1300°C and 2700°C. The elastic modulus of both fibres followed the same trend, increasing with the graphitisation temperature. On the other hand, the tensile strength of these fibres showed the opposite trend, i.e. it increased for ex-MPP CFs and decreased for ex-PAN fibres, with increasing graphitisation temperature. This trend was correlated with the microporosity observed in both fibres, which decreased monotonously for ex-MPP CFs, while it increased for ex-PAN CFs until 2000°C, and decreased moderately at 2700°C.

The different responses of ex-PAN and ex-MPP fibres were attributed to the parent structures and the different transformation paths experienced by each fibre [32]. The MPP parent fibres exhibited ordered stacking of graphene planes and experienced only a minor transformation, releasing small amounts of hydrogen. On the other hand, ex-PAN fibres underwent a profound structural transformation of the parent turbostratic structure, with the evolution of

nitrogen. Consequently, ex-MPP CFs exhibited fewer crystalline defects than ex-PAN CFs graphitised at the same temperature.

Table 1: Crystalline dimensions obtained from HR-TEM images on ex-PAN and ex-MPP carbon fibres [32, 33]

Sample	d_{002} [nm]	$L_C^{\pm}$ [nm]		$L_{a//}$ [nm]	L_{aT} [nm]	Z [°]	$I_T/I_G^{\dagger}$
PAN 1300°C	0.3570	1.5	2.0	4.0	4.3	36.72	0.612
PAN 2000°C	0.3463	3.5	3.5	6.0	9.5	29.70	0.514
PAN 2500°C	0.3430	5.7	5.3	19	12	20.70	0.338
PAN 2700°C	0.3429	7.0	7.0	23	14	19.62	0.271
MPP 1300°C	0.3512	2.6	2.7	5.5	5.0	24.66	0.561
MPP 2000°C	0.3419	8	13	27	20	10.44	0.201
MPP 2500°C	0.3377	18	27	45	33	6.84	0.203
MPP 2700°C	0.3387	23	30	66	36	8.64	0.196
Lignin 1500°C	0.3450	1.0		2.0			
Lignin 2000°C	0.3430	2.1		4.0			

$^{\pm}$Transverse section and longitudinal section
†Results obtained from X-ray diffraction studies

HR-TEM observations of ex-PAN fibres graphitised at 1300°C revealed a turbostratic structure formed by wrinkled and entangled crystallites composed of small graphitic basal planes [32]. With increasing temperature, an isotropic distribution of larger unwrinkled crystallites formed in an overall amorphous structure. Li et al. [34] reported a similar evolution of the microstructure of ex-PAN CFs. On the other hand, ex-MPP CFs exhibited an ordered distribution of graphitic basal planes, without mutual entanglements [32]. The observations on the longitudinal cross-sections revealed a preferential alignment of the graphitic basal planes with respect to the fibre axis. The preferred orientation was more clearly defined in ex-MPP CFs than for ex-PAN CFs, and it increased with the graphitisation temperature in both cases. The crystalline dimensions obtained from the HR-TEM images are summarised in Table 1 [32, 33]. The interlayer spacing (d_{002}), the stacking thickness (L_C) and the crystallite dimensions in the parallel ($L_{a//}$) and transverse directions (L_{aT}), with respect to the fibre axis, increase with

the graphitisation temperature. The faster crystallite growth observed for ex-MPP CFs was attributed to the lack of entanglement, crosslinking and internal stress between ribbons, which makes it easier for layers to stack, collide and bond together. The last columns in Table 1 correspond to the misorientation angle (Z), and the intensity ratio between the disordered turbostratic (I_T) and ordered graphitic (I_G) structures, derived from XRD experiments. The evolution of the microstructure of CFs, with increasing graphitisation temperature, is illustrated in Figure 3.

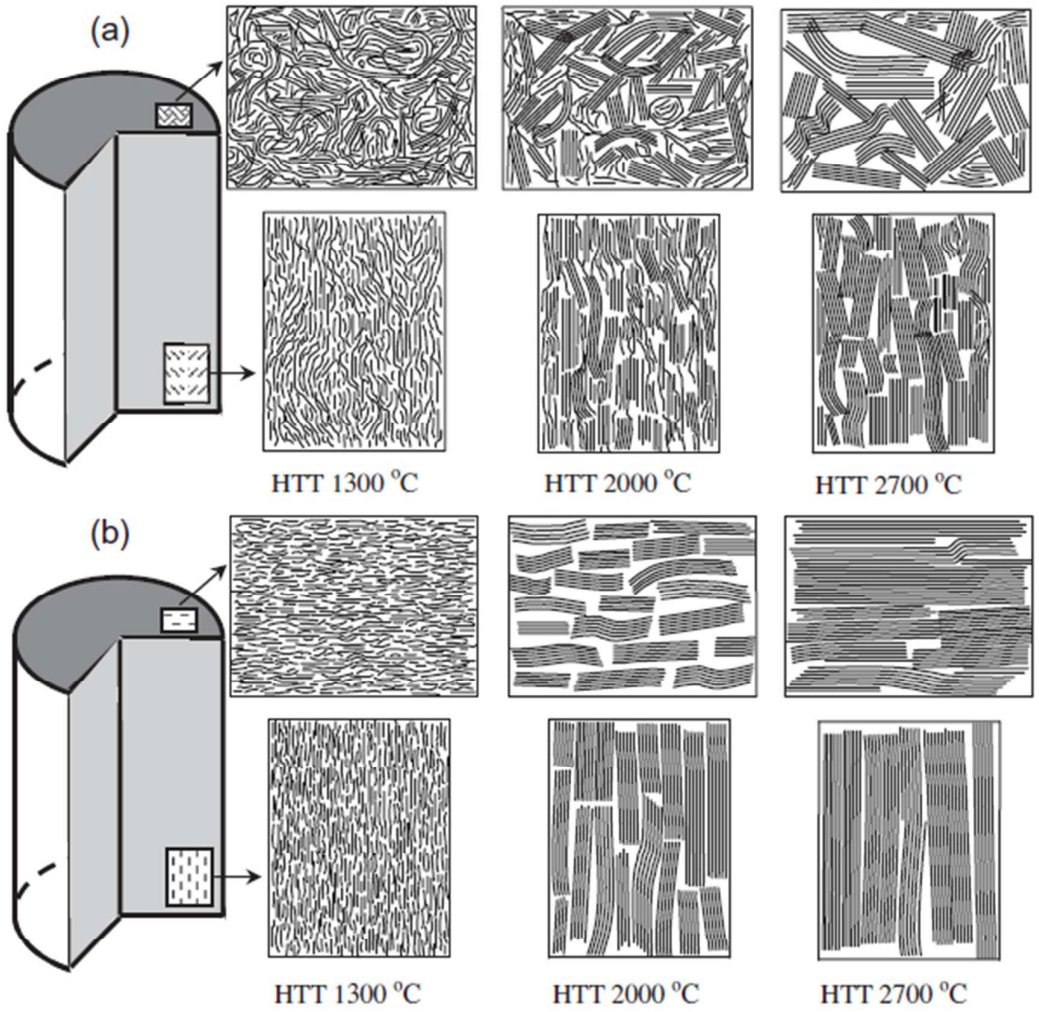

Figure 3: Proposed mechanism for the microstructural rearrangement and crystallite growth in the transverse and longitudinal sections of carbon fibres: a) ex-PAN and b) ex-MPP [32].

More recently, Li et al. [34] reported a strain relaxation of the internal structure of CFs during graphitisation. The authors arrived at this conclusion through a detailed study of the peak shift in Raman spectroscopy and the asymmetric peak shape in wide angle X-ray diffraction (WAXD) measurements. The residual strain and the associated stress present in the entanglements and crystallite defects is said to make the structure of the CFs unstable during heat treatment. In order to relieve the stress, the carbon layers slide and rotate to straighten along the fibre axis into a flat and smooth morphology, thus increasing the axial ratio of the crystallites ($L_{a//}/L_{aT}$). Therefore, the formation of elongated micro-crystals and porosity was linked with the stress relaxation during heat treatment.

2.d. Carbon fibres derived from bio-precursors

Bio-polymers, such as cellulose and lignin, are interesting sources of carbonaceous material because of their abundance and low-cost [35]. Following the early work on cellulose fibres [36], researchers have recently shifted their attention to lignin because it is renewable and environmentally friendly, it does not belong to the human food chain, it can be obtained as by-product from wood pulping and it possesses promising physical and chemical properties for carbon fibre production [35, 37]. However, the spinning, stabilisation and carbonisation of ex-Lignin CFs is a challenging process with a narrow window of operating conditions, involving its glass transition temperature (T_g), chemical stability and cross-linking characteristics [17, 37, 38].

The microstructure of ex-Lignin CFs typically exhibits a dispersion of small graphitised inclusions in an amorphous carbon matrix [33]. The ordered regions are attributed to inorganic impurities, which trigger catalytic graphitisation during heat treatment, whereas the matrix shows a poorly developed lattice structure (Table 1) [24, 33]. The low degree of alignment and

structural heterogeneity of these CFs are responsible for their modest mechanical properties [16, 33, 37]. In spite of this, the interest in ex-Lignin CFs was renewed in recent years as a result of the increasing demand for light and low-cost materials to comply with stringent environmental regulations in the transportation sector [38]. Moreover, advanced characterisation techniques have provided new insights on the microstructural heterogeneity and pore structure of ex-Lignin CFs [39, 40], which is a promising indication of forthcoming breakthroughs in this field.

3. Surface functionalisation: lessons learned from other technologies

The microstructure of CFs influences their response to the surface treatments and, as a result, the complex microstructure contributes to the diverse results reported in the literature. Tang and Karoos [2] mentioned in their review that the low-modulus CFs, such as ex-PAN, exhibit a lower degree of crystallite alignment. Consequently, these fibres have more crystallites intersecting the surface, which represent chemically active sites to react with the treatment medium. On the other hand, the high-modulus CFs, for example ex-MPP fibres, exhibit a high degree of crystallite orientation and a skin structure mainly consisting of graphitic basal planes. In consequence, these CFs are highly inert to the treatment medium. However, a small amount of active sites is always found on defects and singular points along the fibres. These sites represent weak points during a surface treatment, resulting in strong localised attack and pits which may reduce the tensile strength of the fibres.

In this section, the phenomena which occur during surface functionalisation are classified into two types, namely ‘chemical’ and ‘topographic or structural’. The observations from conventional functionalisation technologies are summarised and discussed, in contrast with plasma functionalisation techniques.

3.a. Surface functionalisation: chemistry

The surface chemistry of CFs and their compatibility with the polymer matrix is perhaps the most important factor for the IFSS. The chemistry of the surface affects the surface energy, wettability and reactivity of the fibres [2]. Functional groups, such as -COOH, -OH, -C=O and/or $–NH_2$, increase the hydrophilicity of the CFs' surface, and enhance their reactivity with the polymeric matrix [4, 41]. Polar elements, such as oxygen and nitrogen, are largely removed from the surface of the CFs during the high temperature carbonisation/graphitisation under inert gas. Therefore, these surface functionalities are subsequently replenished by different surface treatments, such as electrochemical oxidation [5, 42], immersion in strong acids [43, 44] or ammonia solutions [4, 45], plasma treatments [20, 41], coatings or sizing [2, 46] with conventional or self-assembly strategies [47], among others.

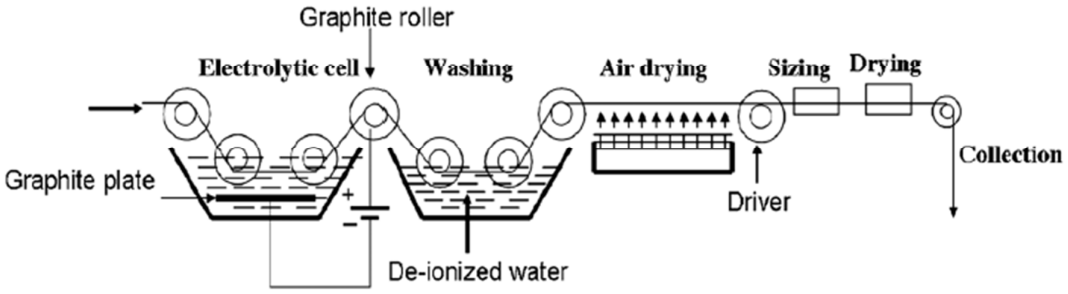

Figure 4: Schematic diagram of the equipment used in [48] for the surface functionalisation of carbon fibres by electrochemical oxidation.

Donnet and Guilpain [5] conducted a systematic study of the electrochemical oxidation of ex-PAN CFs in different solutions and under conditions similar to the ones used in industry (Figure 4). They found that the CFs were subjected to non-homogeneous surface oxidation, as a result of the intrinsic inhomogeneity of the process and the relative position of the individual CFs in the bundle. Furthermore, the electrochemical oxidation had a smoothing

effect on the CFs' surface at the initial stages. However, surface pitting occurred upon increasing the treatment time and the degree of oxidation. This created stress concentration sites on the surface of the CFs, which ultimately reduced their tensile strength.

More recently, Qian et al. [42] studied the electrochemical oxidation of ex-PAN CFs in a NH_4HCO_3 electrolyte, using different current densities. The results of X-ray photoelectron spectroscopy (XPS) revealed the presence of graphitic carbon (-C-C, 284.6 eV), phenolic or hydroxyl groups (-OH, 285.3-285.8 eV), carbonyl or quinone groups (-C=O, 286.3-287.0 eV) and carboxyl or ester groups (-COOH, 288.0-288.8 eV). The –C=O and –COOH groups increased considerably with the current density until a maximum point, and subsequently decreased for higher current densities. The IFSS exhibited a similar response and the trend was correlated with the content of –COOH groups in particular. A drop in IFSS for higher current densities was attributed to the surface saturation with –COOH groups and the relative decrease in their content compared with other functional groups.

Immersion treatments in acid or ammonia solutions are also used to modify the surface of CFs and to increase the density of active groups. Wu et al. [15] conducted a study on the oxidation of ex-PAN CFs in concentrated nitric acid (70 wt.%) at 115°C. They reported increased contents of active groups, mainly carboxylic (-C=O) and hydroxyl (-OH) groups, on the surface of the CFs. The introduction of these polar functionalities was responsible for the increased hydrophilicity of the fibres. However, a reduction in the tensile strength was observed, and this was attributed to the development of pits and crevices upon longer oxidation treatments. Interestingly, low-modulus ex-PAN fibres lost their strength more readily than high-modulus fibres and thus the formation of defects was associated with the microstructure of these CFs, i.e. the authors proposed that nitric acid reacts more readily with the less crystallised regions of the fibre.

Nohara et al. [43] conducted a comparative assessment of the surface treatment of ex-PAN CFs with hydrochloric and nitric acids. In both cases, the surface treatment removed the binder from the surface of the fibres. The attack was heterogeneous, and the CFs at the periphery of the bundle were etched more severely than the ones at its centre. The fibres treated with hydrochloric acid showed little or no signs of roughening, while the fibres treated with nitric acid exhibited apparent changes in morphology and deep crevices. The tensile strength dropped with increasing treatment time, which was attributed to the stress concentration produced by deep crevices formed during etching. The results from Raman spectroscopy proved that the graphitic structure of the CFs remained unchanged after the surface treatment. However, the authors found increased number of functional groups on the surface, particularly on the fibres treated with nitric acid [43, 44].

Pamula and Rouxhet [49] characterised the surface of low-modulus ex-PAN CFs oxidised in boiling nitric acid (68 wt.%) for 1 hour. The fibres exhibited increased roughness or microporosity after the oxidation treatments. More importantly, they became hydrophilic upon oxidation and this was attributed to the large increase in the content of oxygen and hydrogen groups (OH, COOH), as well as the modification of the nitrogen-containing functional groups. Interestingly, the total oxygen concentration was found to be too high to be accounted for by the external surface only. Therefore, the authors proposed a swelling mechanism by which the whole fibre, rather than just its surface, becomes accessible to the chemical reagents.

More recently, Vautard et al. [50] conducted an extensive study on the oxidation of intermediate-modulus ex-PAN CFs in nitric acid under similar conditions. The diameter of the fibre was found to remain unchanged after the oxidation treatment, but the authors described a significant change in the surface roughness. The formation of a network of micropores could not be confirmed by the absorption analysis, although the authors compared

XPS and temperature programmed desorption (TPD) results and concluded that a considerable amount of functional groups were present well below the surface of the fibre. The effect of the surface functionalities on the IFSS was emphasised, in relation with the matrix curing conditions.

In their article, Langston and Granata [51] provided a summary and critical discussion of the existing evidence on nitric acid oxidation of CFs. The authors linked the oxidation process with the microstructure, and emphasised the effect of the highly ordered microstructure of high-modulus fibres on their low reactivity to the surface treatment compared to high-strength fibres. In a similar way, the skin and the core of a fibre respond differently to the treatment in view of their microstructural differences. More importantly, the tensile strength of the fibres increased after oxidation, which was attributed to the removal of the surface layer containing residual stresses and defects.

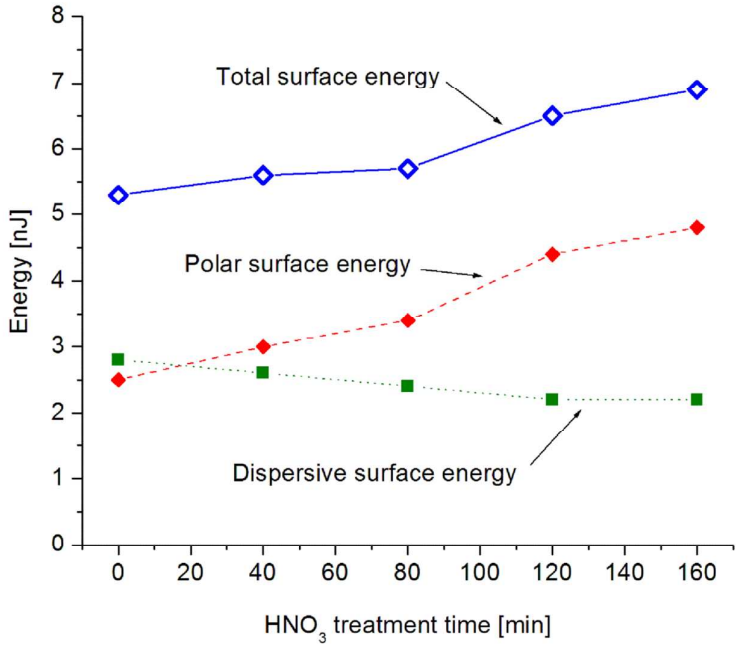

Figure 5: Surface energy of carbon fibres functionalised with nitric acid as a function of the treatment time [51].

With regards to the surface chemistry, Langston and Granata [51] observed an increase in the oxygen content and this was associated with a higher surface concentration of carbonyl (-C=O) and carboxyl (-COOH) groups. The content of hydroxyl groups (-OH) declined after the oxidation treatment. The increase in the concentration of carbonyl and carboxylic acid increased the surface energy of the fibres, particularly the polar component (Figure 5). On the other hand, the dispersive component of the surface energy dropped with treatment time, and this was attributed to the increase in surface oxidation, and the lower polarisability of the electronegative oxygen atoms. Once the surface of the CFs was saturated, subsequent increases in the content of active groups took place by creation of microroughness and microporosity.

As alternative to the oxygen containing functional groups, it is well known that amino groups ($-NH_x$) react rapidly with epoxides and isocyanates in the polymeric matrices, increasing the IFSS in epoxy resin/CF composites. Pittman et al. [12] studied the oxidation of ex-PAN CFs in nitric acid followed by reaction with tetraethylenepentamine (TEPA) to attach amino groups ($-NH_x$) to the carboxyl groups (-COOH). More recently, Severini et al. [4] studied the surface treatment of CFs in ammonia solutions at different times and temperatures. They confirmed the presence of $-NH_x$ groups on the surface, which were associated with an increase in the bond strength of CFs embedded in epoxide composites. Other authors confirmed the increase in the nitrogen and oxygen content, but the clear identification of the chemical state was hindered by the overlap of the peaks in the XPS spectra [52].

On the other hand, a similar study conducted by Song et al. [45], revealed no new functional groups on the surface of the ex-PAN CFs after a surface treatment with ammonia. The changes in wettability and in bond strength were attributed to the surface roughness and the mechanical interlocking respectively, rather than to changes in the surface chemistry. The

authors identified residues of the binding agent on the fibres, even after the surface treatment. Binders are typically sprayed on commercial CFs to protect them during handling operations [45], and their formulation is often a trade secret. Some binders may be difficult to remove without damaging the fibres, and this is one of the factors contributing to the inconsistent results found in the literature [53, 54].

Jones and Sammann [55] studied the effect of low-power plasma surface treatments of ex-PAN CFs in air, N_2-H_2 and argon. They used a low power (< 1 W) radio frequency (RF) source to sustain the plasma in a small tube. The XPS studies revealed some changes in the surface chemistry of the CFs. The fibres treated in air showed equivalent results to the wet electrochemical treatments in aqueous solutions, with a detectable increase in the oxygen content. The fibres treated in argon also showed high oxygen content on the surface, which was attributed to the pick-up of residual oxygen from the vacuum chamber. In addition, the argon plasma degraded the properties of CFs, even after very short treatment times. Finally, the plasma treatments with ammonia resulted in greater amounts of nitrogen functional groups and no oxygen on the surface of the fibres. This was considered beneficial for the bonding of the CFs with epoxy resins.

Montes-Morán et al. [56] studied the effect of oxygen plasmas on ex-PAN and ex-MPP CFs, using a microwave generator (75 W) to sustain the oxygen plasma at 100 Pa pressure. The topography of the CFs showed no considerable alterations after the surface treatment and the IFSS increased in all cases. This was attributed to the surface functionalisation on the CFs, and the enhanced adsorption of polar molecules by acid-base interactions. On the other hand, a similar study conducted by Cioffi et al. [57] resulted in clear reductions in the tensile strength of CFs exposed to argon and oxygen plasmas. These authors used a RF source (50 W) to sustain argon and oxygen plasmas at 40 Pa, from 5 s to 100 s. The reduction in the tensile strength of the fibres was attributed to the increased roughness and the formation of surface

defects as a result of the sputtering action of argon ions, and the sputtering and etching action of oxygen species [58].

Mao et al. [59] used an electron beam (EB) irradiation technique to functionalise CFs with dimethylenetriamine (DETA) and triethylene tetramine (TETA) solutions at difference concentrations. The EB technique was said to offer a simpler, more effective and environmentally friendly pathway to graft amino groups onto the surface of CFs. The authors confirmed the presence of amino groups (-NH_x) by XPS. As the concentration of NH_x groups increased, the content of carboxyl (–COOH) and carbonyl (-C=O) groups decreased. The Raman spectroscopy results revealed an increase in the degree of disorder for most of the treated CFs. In addition, treated fibres exhibited increased roughness. Therefore, the increase in IFSS was attributed to the combination of three factors: improved chemical bonding with NH groups, higher adsorption interaction with the disordered carbon structure, and increased mechanical interlocking with the rough CF surface.

To the best of our knowledge, no systematic study has been published yet on the surface functionalisation of ex-Lignin CFs. Based on their high degree of disorder and density of pores and defects, it is expected that these CFs will be prone to localised chemical attack, leading to a rapid drop in tensile strength. Therefore, we anticipate that the CFs derived from bio-precursors will require milder processing conditions than their conventional ex-PAN and ex-MPP counterparts.

3.b. Surface functionalisation: topography and structure

The surface topography of CFs is frequently associated with the IFSS in two ways: increased surface area and mechanical interlocking [2]. The increase in roughness expands the available surface area for the attachment of active groups, thus increasing the interaction with the polymer (Figure 6). Moreover, the pits and crevices provide mechanical interlocking sites for

the matrix. However, these defects also act as stress concentrators and frequently reduce the tensile strength of the fibres. Pits and crevices are preferentially developed at disordered areas of the surface, where carbon atoms with dangling bonds offer preferential sites for the reactions, compared with the inert basal planes.

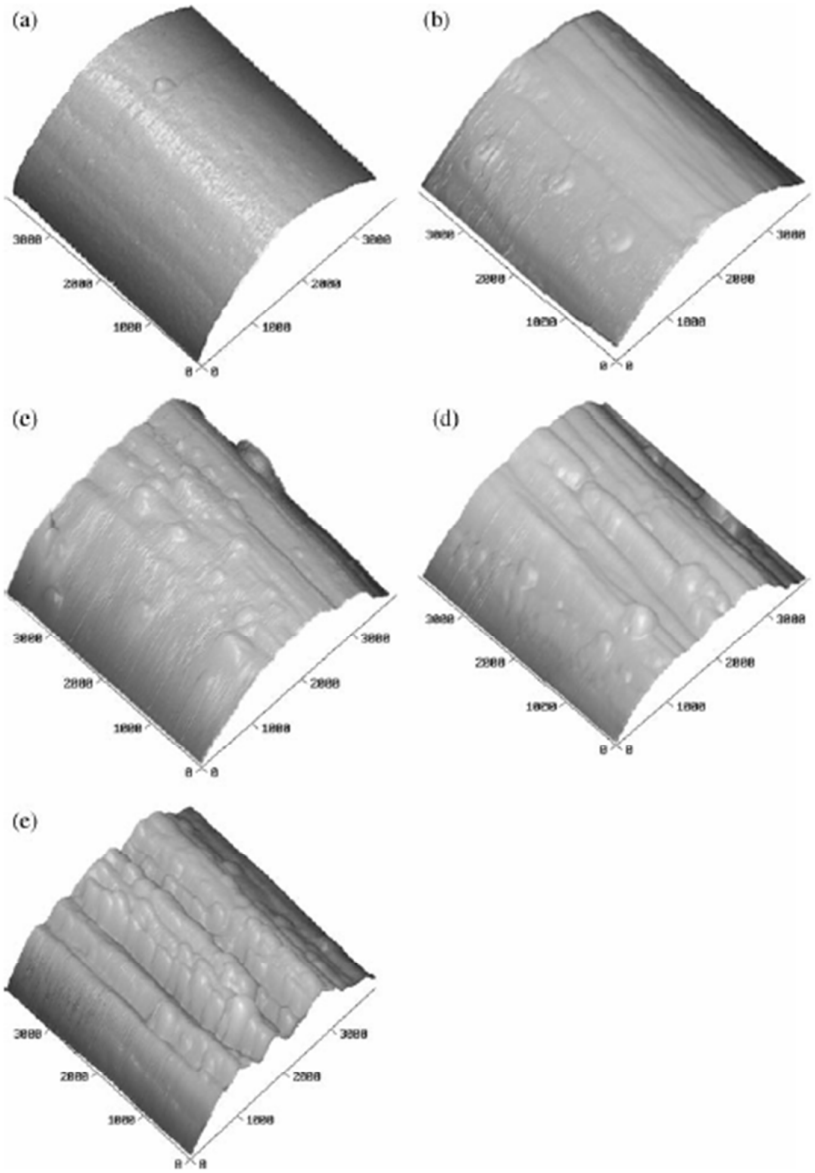

Figure 6: AFM surface profile of carbon fibres after plasma treatments with increasing time: a) untreated, b) 5 c) 10 d) 15 and e) 20 minutes [58].

In a study on surface oxidation of CFs with nitric acid, Pittman et al. [12] reported preferential oxidation of lateral graphitic planes intersecting the surface, compared with the slower oxidation of highly ordered basal planes. These authors proposed a mechanism by which the preferential oxidation opens pre-existing voids present in the subsurface of the CFs (Figure 7). As the oxidation proceeds, the voids are exposed to the surface, thus accounting for the observed pits and crevices. The exposure of pre-existing voids increases the surface area, which explains the large increase in the content of active groups observed upon progressive oxidation.

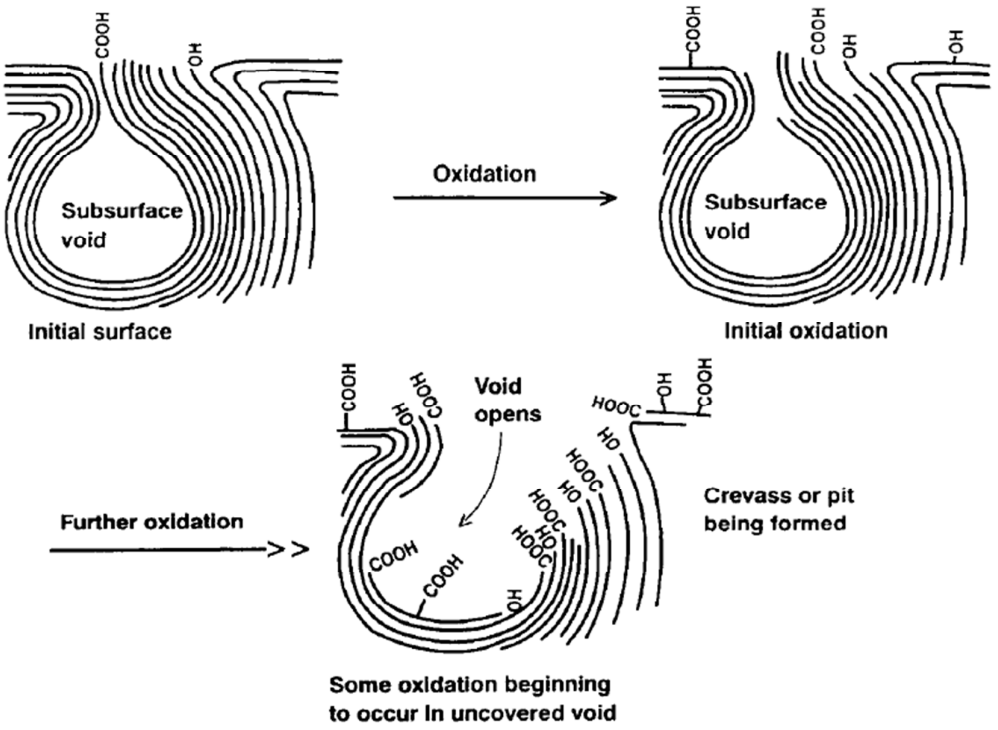

Figure 7: Proposed mechanism for the preferential oxidation which occurs at surface defects during functionalisation of carbon fibres with nitric acid [12].

Solís-Fernández et al. [6] conducted a comparative study of physical and chemical oxidation mechanisms of highly ordered pyrolytic graphite (HOPG). Their results revealed interesting differences between the physically and chemically driven oxidation of HOPG surfaces in the gas phase, using ultraviolet oxidation (UVO) and dielectric barrier discharge (DBD) oxidation. They distinguished between two operating mechanisms: a chemically driven attack, based on the active species from the oxidative medium (UV oxidation), and a physically driven attack, through electric discharges and bombardment of the surface with energetic charged species or ions (DBD oxidation).

The etching rate of UV oxidation was considerably lower than the DBD oxidation, and the attack was localised on surface defects forming monolayer-deep pits [6]. The pits grew laterally and new pits nucleated until they merged, after long oxidation times, exposing a new layer of material. On the other hand, the DBD oxidised samples showed evidence of plasma induced attack in localised areas, approximately 400 μm in diameter. These areas were said to be the footprints of individual electric discharges (filaments) and they exhibited an atomically rough morphology, with depressions and protrusions attributed to microstructural defects. After extended treatment times, the full surface of the sample became uniformly covered by these footprints, although there was a trend toward re-strike of a filament on the same point due to a charge accumulation effect.

The chemical attack was a highly selective process, restricted to high energy sites (vacancies, step edges, grain boundaries, etc.) where carbon atoms are readily available to react with oxidising species. On the other hand, the physical attack observed in DBD was a non-selective process, which created ion-induced defects across the surface with equal probability [6]. A very similar mechanism was reported by Yang et al. [60] for graphene exposed to a hydrogen plasma, generated by low RF power (50 W and 100 W). The chemical attack dominated at low RF power, and proceeded by hydrogenation and volatilisation of carbon

atoms at defect sites. Increased RF power resulted in stronger plasma etching and created more defects on the graphite basal planes.

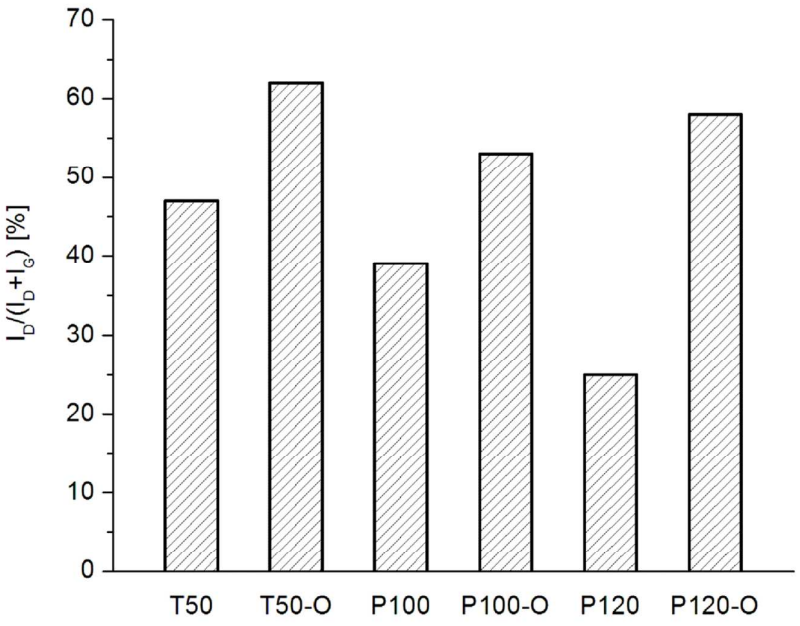

Figure 8: Structural order parameter $I_D/(I_D+I_G)$ of untreated and plasma oxidised (O) carbon fibres [61].

Note: T50 is an ex-MPP carbon fibre, while P100 and P120 are ex-PAN carbon fibres.

Montes-Morán et al. [61] used wide angle X-ray diffraction (WAXD) and Raman spectroscopy to study the effect of plasma surface oxidation on the graphitic structure of the CFs. The diffraction traces obtained at different fibre orientations were used to calculate the interlayer spacing (d_{002}), the stacking thickness (L_c) and crystallite dimensions (L_a) of the graphitic crystallites, as well as to identify peaks corresponding to the turbostratic structure. The results revealed differences between the original fibres, ex-PAN and ex-MPP, but no changes were detected after the plasma treatment. In the case of Raman spectroscopy, the position of the main Raman bands remained unchanged before and after the plasma treatment. However, the

intensity ratio between the first-order D and G bands ($I_D/(I_D+I_G)$) increased consistently after the plasma oxidation treatment (Figure 8). The D band was associated with the presence of defects, the disruption of the basal planes and the creation of edge carbon planes, whereas the G band corresponded to the ordered graphitic structure. Therefore, the plasma treatment produced an increase in the structural disorder on the surface of CFs, while the bulk of the fibre remained unaffected.

Akbar et al. [62] reported similar results for CFs treated in nitrogen RF plasma, i.e. an increase in the disorder of the graphitic structure on the surface of the fibres. Furthermore, these authors mapped a wide range of treatment conditions, including low-frequency power, high-frequency power, gas pressure and time. They observed a non-linear relationship between the processing conditions and the changes in I_D/I_G, which was attributed to changes in the plasma regime. Unfortunately, no plasma characterisation technique was used in this study to quantify plasma parameters, such as electron temperature, electron density, ion energy and ion flow. As a result, the interpretation of the data was rather cumbersome, although it is possible to extract some qualitative trends.

The high frequency power (40.68 MHz, HF) was correlated with the ion flux, whereas the low frequency power (2.1 MHz, LF) was said to affect ion energy [62]. At the same time, it is known that the gas pressure affects the mean free path between collisions and the collision probability. Therefore, high RF power (both HF and LF) and low gas pressure would favour energetic ions, capable of introducing defects in the graphitic structure, even at low ion fluxes. These conditions were vaguely associated with higher I_D/I_G ratios, i.e. higher degrees of disorder. On the other hand, low power and high pressure would favour low energy ions and higher ion fluxes with a smaller impact on the graphitic structure.

Akbar et al. [62] also observed a complex trend in the I_D/I_G ratio as a function of time. This could be attributed to more subtle differences in the plasma regime and in the plasma-surface

interactions, particularly the removal of weakly bonded layers from the surface. In a related article, Tang et al. [63] conducted a comparative study on the effect of atmospheric- (APP) and low-pressure plasmas (LPP) on poly(methyl methacrylate) plates. The plasma was ignited using an RF power source and argon as a treatment gas in both cases. The authors reported that APP produced more noticeable changes in the roughness and in the surface morphology of the treated samples. This was associated with the higher discharge density and the sharp temperature cycle created by APP, in contrast with the low etching effect produced by the ion bombardment in LPP.

With regards to ex-Lignin CFs, it is difficult to predict the dominating plasma-surface phenomena without experimental evidence. However, it is expected that the disordered microstructure of these CFs would respond better the non-selective nature of the LPP surface functionalisation, as well as the mild surface roughening produced by low energy ion bombardment. These surface treatments are likely to improve the IFSS without reducing the strength of ex-Lignin CFs excessively.

3.c. Comparative studies

Jang et al. [64] compared the IFSS and flexural strength of composites produced with ex-PAN CF treated with 65 wt.% nitric acid at 100°C and RF oxygen plasma (13.56 MHz and 100 W). Regarding the treatment time, the authors found the best results for 60 minutes treatment with nitric acid and 3 minutes treatment with RF oxygen plasma. Both techniques increased the roughness and the surface area of the CFs. However, the Brunauer–Emmett–Teller (BET) surface area calculations revealed that the fibres treated with nitric acid had larger surface area than their plasma treated counterparts. The XPS measurements indicated similar O/C ratios in both cases. The authors concluded that nitric acid treatments were more effective than oxygen plasma treatments to increase the mechanical properties of CF composites. This

would indicate that the surface roughness had a dominant effect on the IFSS compared to the surface chemistry. However, a reduction in mechanical properties was noted upon long surface treatment times, which was attributed to the degradation of the fibres owing to localised chemical attack.

Nohara et al. [43] conducted a similar study on ex-PAN CFs treated with hydrochloric and nitric acids at 103°C, and argon and oxygen plasmas (40 Pa, 1 A and 100 V). Unfortunately, the authors did not describe the plasma discharge system in detail. Moreover, the fibres were treated in the as-received condition, i.e. without removing the binding agent. All surface treatments degraded the tensile strength of the fibres after long exposure times (20 minutes). The degradation was faster for nitric acid than for hydrochloric acid, the argon plasma produced a similar degradation, whereas the oxygen plasma treatment reduced the tensile strength severely. This was attributed to the oxidation of the fibres on active sites, with the following progression: C-OH, C=O, COOH and finally CO_2.

The study of the surface topography [43] revealed that all the surface treatments removed the binder, as well as the outermost layer of the CFs. A smoothing effect was observed for acid treatments, and this was more pronounced for nitric acid than for hydrochloric acid. On the other hand, argon and oxygen plasma treatments increased the roughness of the fibres by deepening the original grooves and creating new ones. The plasma treated fibres showed signs of redeposition of sputtered material, but no changes in the graphitic structure were detected. The XPS results indicated that all the treatments increased the O/C ratio of the fibres, with the exception of the argon plasma treatment. The O/C ratio was highest for the nitric acid treatment, followed by the hydrochloric acid, the oxygen plasma and the argon plasma treatment.

In Ref. 55, it was suggested that the quantification of active groups by XPS (and other techniques) may include functional groups which are not accessible to the resin when

manufacturing a composite material. Therefore, a correlation of the content of functional groups with the IFSS may produce misleading results. This observation is particularly important when comparing plasma treatments with wet chemical methods, because the effect of the former treatments is strictly limited to the surface, while the latter introduce active groups in the subsurface of the fibres as well [49, 50]. In addition, a degradation of the functionalised surface upon exposure to atmospheric conditions was attributed to the physisorption of gases and moisture [55]. The surface treatments conducted under vacuum would be particularly sensitive to this degradation mechanism. On the other hand, some unstable functional groups introduced by wet chemical methods may evolve and desorb from the CF surface under the high vacuum used for XPS measurements [65, 66]. Therefore, care should be exercised when interpreting and quantifying the results.

Table 2: Typical properties of surface functionalised ex-PAN carbon fibres

Surface treatment	Functional groups	Filament strength*	Interlaminar shear strength*	Ref.
Electrochemical oxidation	C-OH, C=O, O-C=O	-15% to 0%	0% to +25%	42, 46, 48
Nitric oxidation	COOH, C=O, NH_x	-15% to +20%	+15% to +45%	15, 50, 51
Aqueous ammonia	COOH, C-NH_x	-20% to 0%	+5% to +50%	4, 45, 52
Atmospheric plasma	COOH, C=O	-15% to 0%	+40% to +70%	67-69
Low pressure plasma	COOH, C=O, NH_x	-12% to 0%	0% to +13%	56, 64, 70

* Relative to the untreated fibres; the range of values reflects different treatment conditions.

The comparative study by Tiwari and Bijwe [44] assessed the surface treatment of ex-PAN CF with nitric acid (15-180 min, 65 wt.% at 110°C), cold remote N_2-1% O_2 plasma, gamma radiation (Co^{60} source, 100-300 kGy doses) and YbF_3 nanoparticles (sonication in ethanol with 0.1-05wt.%). The assessment included the fibre-matrix adhesion, tensile strength, surface roughness, surface functional groups and C structure of the fibres, followed by the mechanical and tribological properties of the resulting composites. The authors concluded

that no treatment improved all the assessed properties at the same time, and the effect was dependant on the type of treatment and its dose. However, the plasma treatment increased the IFSS with the least influence on the tensile strength of the fibres and minimum effect on the turbostratic structure (Table 2). Hence, the plasma technology is a promising candidate for the surface treatment of carbon materials with a disordered microstructure.

4. Plasma technologies for surface treatment of carbon fibres

The plasma treatment of engineering fibres has received increasing attention because of environmental and technical reasons [71]. From the environmental point of view, the plasma technology is clean and offers advantages over wet chemical methods [20]. From the technical point of view, plasma treatments, particularly non-thermal plasmas, are versatile and can introduce changes in the surface chemistry of the CFs without affecting their bulk mechanical properties. The results reported in the literature show a large scattering, which is a reflection of the wide range of plasma techniques, experimental set-ups and operating conditions. Authors typically report alterations in the surface chemistry depending on the gas species, changes in the graphitic structure as a function of the ion energy, and variations in surface roughness depending on the gas mixture, the applied power and the treatment time.

Various plasma techniques have been applied to the surface modification of CFs, including: Dielectric Barrier Discharge (DBD) [67], Corona Discharge (CD) [72], Radio Frequency (RF) [64], Microwave (MW) [56], Direct Current (DC) plasmas [20] and Plasma Immersion Ion implantation (PIII) [73] (Table 3). Atmospheric plasmas, such as DBD and CD, are convenient because the treatments are conducted under atmospheric pressure and they are easier to integrate with continuous production lines. On the other hand, RF, MW and DC plasmas are typically conducted in vacuum, which involves additional challenges and costs. However, low pressure

plasmas are an interesting option for the high-end sectors, where the performance outweighs the additional costs [41].

Table 3: Plasma technologies and surface interaction mechanisms

Method	Gas pressure	Effect on		IFSS mechanism	Ref
		Roughness	Filament strength		
Microwaves (MW)	Vacuum	↑	↓	Chemical	20, 56
Radio Frequency (RF)	Vacuum	↑↑	↓↓	Chemical-Physical	20, 64
Plasma immersion ion implantation	Vacuum	↑↑	↓↓	Chemical-Physical	73
Direct Current (DC)	Vacuum	↑↑↑	↓↓↓	Physical-Chemical	14, 20
Dielectric barrier discharge (DBD)	Atmospheric	↑↑↑↑	↓↓↓↓	Physical-Chemical	6, 67
Corona discharge (CD)	Atmospheric	↑↑↑↑↑	↓↓↓↓↓	Physical	20, 72

* The severity of the plasma treatment depends on the power level and the gas mixture

The type of plasma technique and the operating conditions determine the dominant physico-chemical phenomena and the plasma-surface interactions. In the plasma state, energetic ions and electrons coexist with relatively cold gas molecules. The temperature difference between the gas molecules and the energetic species is mainly determined by the mean free path between collisions, which is a function of the gas pressure. The atmospheric plasmas are characterised by frequent collisions. These types of plasmas are often called *hot plasmas* because the gas temperature may be as high as 10,000 K [20]. The high temperature and, usually, the high energy density are very effective for roughening the surface of CFs. However, these treatments need to be conducted at high speeds (~10^{-3} s) to avoid damage on the fibres.

On the other hand, low pressure plasmas are normally termed *cold plasmas* because the low collision frequency results in a gas temperature well below 1,000 K, typically 300 K [20]. Under such conditions, ions and excited species can travel longer distances between collisions, and the CFs exposed to the plasma are subjected to a low-energy ion

bombardment. However, as it is illustrated in Figure 9, the energy level of ionised species in the plasma is higher than the chemical bond strengths in the CFs. Therefore, the interaction of these energetic species with the CFs is capable of triggering chemical reactions and structural changes, even though the temperature of the gas remains low. The extent of such surface modification depends strongly on the microstructure of the CFs, the nature of the gas species and the plasma conditions [70].

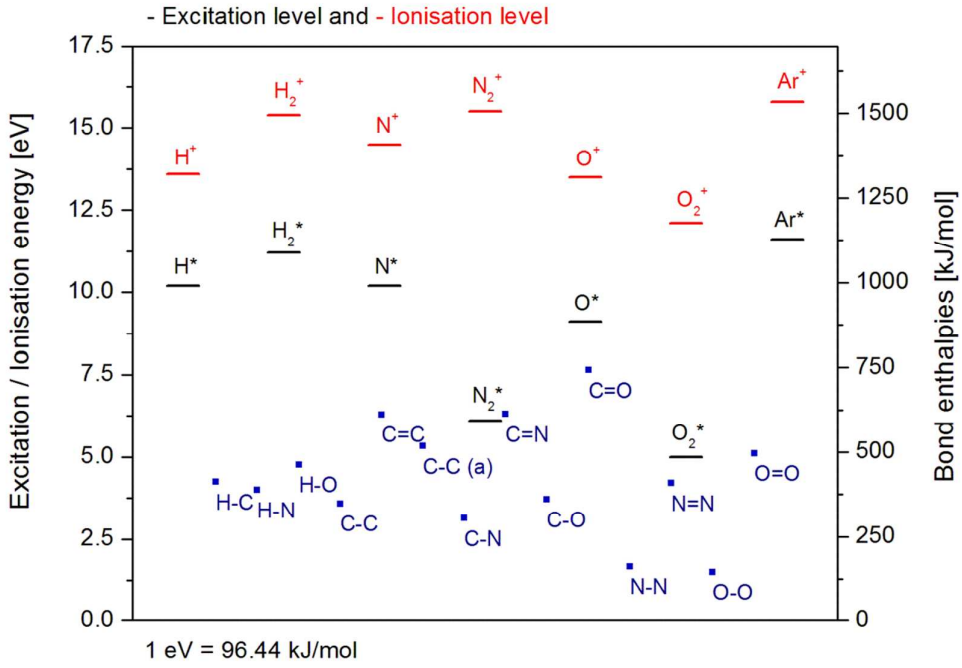

Figure 9: Illustration of the energy levels of active species in the plasma and the strength of chemical bonds found in carbon fibres. Data from [74, 75].

4.a. Low pressure plasmas

Among the low pressure plasma techniques, conventional DC plasmas or glow discharges are very simple, but they can only be applied to conductive materials. In contrast, RF and MW plasmas are adequate to modify the surface of non-conductive materials, but the equipment

tends to be more sophisticated and expensive [20]. The literature shows a wide range of processing conditions but, most typically, air, oxygen, nitrogen, argon, ammonia gases are used [70] at operating pressures between 1 Pa and 100 Pa. The applied power is usually below 300 W and the temperature is kept below 150°C [20]. RF frequencies are normally in the order of tens of MHz (mostly 13.56 MHz), whereas MW frequencies are in the GHz range (mainly 2.45 GHz). These surface treatments are said to remove contaminants from the surface of CFs, introduce active groups, roughen the surface, while leaving the tensile strength virtually unaltered [2].

Unfortunately, a comparison of the different plasma treatments is very difficult because the operating conditions vary considerably; in some cases, the description of the apparatus is insufficient; and, in most cases, the plasmas are described by extrinsic parameters (power, voltage, gas pressure) rather than by intrinsic plasma conditions (electron temperature, electron density, ion energy and ion flow, etc.). The intrinsic plasma conditions determine the type of plasma-surface interactions, which are mainly chemical phenomena driven by active species in the plasma, or physical phenomena triggered by the bombardment with energetic ions. The following section explores these two main mechanisms in low-pressure plasmas and their influence on the surface of CFs.

4.b. Chemical interaction between plasma species and carbon fibres

Jones and Sammann published two articles [13, 55] on the effect of low power nitrogen, air, ammonia and argon plasmas on ex-PAN and ex-MPP CFs, as well as on highly oriented pyrolytic graphite (HOPG). In Ref. 13 the authors found that the ex-PAN fibres responded more readily to the surface treatments than their ex-MPP counterparts. The ex-MPP CFs, with a more organised microstructure, reacted to the plasma treatment in a similar way to HOPG. It was concluded that the chemical modification took place on the edge sites and on

defects, rather than on basal planes. With this regard, a mild ion bombardment of the CFs had positive effects, by generating new defects and active sites. This was produced by electrically biasing the fibres negatively with respect to the plasma potential.

Jang [70] conducted a study on ex-PAN CFs surface treated with oxygen, argon, nitrogen, and ammonia RF plasmas, between 1 minute and 35 minutes. The oxygen and argon plasmas had similar etching power but lead to different levels of IFSS. It was concluded that the surface roughness was a contributing factor to IFSS, but the higher bond strength observed after oxygen plasmas was attributed to the introduction of oxygen functional groups (C-OH, C=O and COOH). On the other hand, ammonia plasma treatments had very minor effects on the surface roughness of the CFs, but the increase in surface energy and in IFSS was remarkable. Moreover, further increases in IFSS were obtained when treating the CFs in a gas mixture of ammonia and argon. The improvement was attributed to the roughening produced by the bombardment with Ar ions, rather than to an additional increase in the number of -NH_x functional groups. Interestingly, the surface energy changed with the treatment time in a non-linear way, but no explanation was offered by the authors [70].

Boudou et al. [76] studied the modification of unsized ex-MPP CFs with oxygen MW plasma. The severity of the treatment was modulated by changing the applied power and the treatment time. Low power and short treatments were dominated by chemical reactions, whereas high power and long treatments were increasingly influenced by physical phenomena related with ion bombardment. Scanning electron microscopy (SEM) observations, conducted on the plasma treated fibres, showed a clean surface with no significant changes in morphology. On the other hand, scanning tunnelling microscopy (STM) images revealed subtle changes in the surface topography of the plasma treated CF, which exhibited a rougher surface with increasing treatment severity. With regards to the surface chemistry, the concentration of oxygen functional groups was associated with the micro-roughness and the microporosity of

the CFs, which provided active sites for the chemisorption of oxygen species. The concentration of oxygen species reached a saturation level early in the plasma process, and no further increase, or even a decrease, in mechanical properties was observed upon extending the treatment time or increasing the applied power. This trend was attributed to the changes in the micro-roughness and the microporosity produced by the ion bombardment.

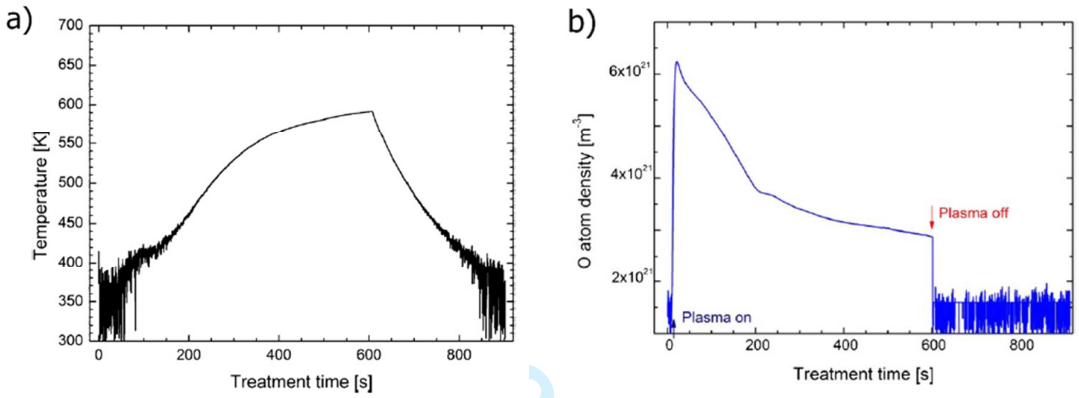

Figure 10: Parameters measured during the RF plasma treatment of sintered graphite: a) temperature of the substrate and b) concentration of oxygen atoms in the plasma [77].

Cvelbar [77] recently studied the interaction of non-equilibrium oxygen RF plasmas with sintered graphite. In addition to the standard physical and chemical characterisation techniques (contact angle and XPS), this author conducted in-situ measurements in the plasma environment, using a double electric probe to measure the concentration of charged species (O^+), a catalytic probe to identify neutral species (O), and an infrared (IR) technique to measure the sample temperature. The samples treated for up to 20 s exhibited a rapid decrease in the contact angle and an increase in the concentration of oxygen groups. Upon longer treatment times, the contact angle remained unaffected or decreased slightly, whereas the number of oxygen functionalities decreased markedly. More importantly, Cvelbar [77] reported a correlation between the density of neutral oxygen atoms in the plasma, the

temperature of the sample and the resulting oxygen functionalities on the surface of graphite (Figure 10). Under these experimental conditions, it was estimated that the sample temperature depended more strongly on the energy released by recombination of neutral oxygen atoms, than on the energy released by ion bombardment. The concentration of oxygen atoms in the plasma quickly dropped in the first 240 s of plasma treatment, and this was accompanied by a marked increase in the temperature of the sample. The author speculated that the increase in temperature destroyed some of the less-stable bonds, while only a small portion of the functional groups remained unaffected. However, the saturation with functional groups could be restored after cooling the sample to room temperature and exposing it to the plasma environment once again, for less than 30 s.

Taking into account that ex-Lignin CFs exhibit a large number of graphitic planes intersecting the surface, short and low-power plasma treatments with mild-etching gas mixtures, such as ammonia or N_2-H_2 mixtures, are expected to produce better results than high energy plasmas or oxidative gas mixtures. The large number of dangling carbon bonds present on the surface of ex-Lignin CFs are likely provide enough active sites for the attachment of functional groups formed in the plasma, rendering ion etching unnecessary or even detrimental for the mechanical properties.

4.c. Physical interaction between plasma species and carbon fibres

The etching effect of argon and oxygen plasmas on the surface of CFs is well known. In most cases, the typical grooves observed on the surface of pristine CFs become visibly deeper and/or they split into more grooves, closely spaced, after the plasma treatment [14]. Yuan et al. [14] also reported that the severity of the etching depends on the degree of graphitisation of the CFs and on the gas species in the plasma. High strength CFs (ex-PAN), with a lower degree of graphitisation, are typically etched more readily than the high modulus (ex-MPP) CFs,

with a highly ordered graphitic structure. At the same time, argon plasmas produce similar or more severe etching than oxygen plasmas, indicating that the etching effect is based on physical phenomena (sputtering) rather than on chemical reactions (oxidation).

The sputtering yield depends on the mass of the incoming ions, the energy of the ions, the angle of incidence, and the surface condition of the target (the CFs in this particular case). In a study on sputtering of carbon substrates (glassy carbon, polycrystalline graphite and diamond), Sugai et al. [78] reported that the sputtering yield was higher at low incidence angles, but it seemed to be insensitive to the condition of the substrate. If CFs can be expected to follow a similar trend, the deepening of the grooves observed upon argon plasma treatments would be related with a shallower incidence angle on the flanks of the grooves, relative to the adjacent surfaces. However, this mechanism would not explain the generation of new grooves, which must involve local differences in the microstructure exhibiting an uneven response to the ion bombardment [14].

In addition to the surface roughening effect, the ion bombardment is known to induce changes in the surface structure of the CFs. The results of Raman spectroscopy reported by Montes-Morán and Young [61] indicate an increase in the $I_D/(I_D+I_G)$ ratio after oxygen plasma treatment. This phenomenon was attributed to the creation of new edge planes, a reduction in crystallite size or the formation of an amorphous carbon layer. Sharma et al. [79] found similar results, i.e. a change in the intensity of the D and G bands, after an oxygen-nitrogen plasma surface treatment, attributed to a decrease in the structural order.

To this end, the response of ex-Lignin CFs to the physical interaction with LPP remains unknown. It is inferred from previous observations that the physical activation mechanisms, such as ion etching, would not be required because the dangling carbon bonds naturally present on the surface of ex-Lignin CFs are expected to provide appropriate active sites for the attachment of functional groups formed in the plasma. Moreover, the highly reactive

surface of ex-Lignin CFs is likely to be prone to excessive damage by localised physical or chemical etching, with detrimental consequences for their mechanical properties. Therefore, the surface treatment conditions will require a careful tunning of the physical and chemical interactions between the ex-Lignin CFs and the LPP environment for optimum results.

5. Summary and future trends

From the previous statements, it becomes apparent that low pressure plasma techniques show great potential to modify the surface of CFs. These treatments are versatile and a careful selection of the processing conditions can optimise the physical and chemical mechanisms dominating the plasma-surface interaction, namely chemical reactions and ion bombardment. The use of plasma diagnostic tools would provide new insights into the plasma conditions and the resulting changes on the CFs. Furthermore, the optimisation of the treatment conditions should consider the dynamic nature of the process, in which the temperature, the surface chemistry and the surface morphology evolve rapidly with time.

The plasma environment introduces new functional groups on the surface of CFs. The changes in the surface chemistry are strictly limited to the outmost layer of the fibres, which is accessible to the polymer when producing composite materials. No functional groups are detected in the subsurface of plasma treated fibres, as opposed to the wet chemical methods. Therefore, a direct comparison of these two methods, based on the quantification of functional groups, should take this phenomenon into account. Furthermore, the decay or degradation of the functional groups after low-pressure plasma treatment, upon exposure to the atmosphere or under the conditions used for characterisation, should also be born in mind and assessed carefully.

The effect of the mild ion bombardment produced by low pressure plasma treatment on CFs is threefold. In first place, it cleans the fibre from adsorbed contaminants and removes weakly

bonded layers of material from the CF surface. In addition to this, the increase in structural disorder generates new active sites for the attachment of functional groups, which increase the surface energy and the wettability of the CFs. Finally, the bombardment with energetic ions can affect the surface microroughness and uncover subsurface microporosity, which increase the interlocking effect with the polymer in composite materials. Consequently, conditions favouring a moderate bombardment by active species would be beneficial, although this should be carefully controlled to avoid excessive damage of the fibres and a reduction in their tensile strength.

A better understanding of the CF microstructure and its effect on the plasma-surface interaction would be most revealing, particularly with the development of new carbon fibres derived from bio-polymers. This applies to the creation of a surface topography by ion etching as well as to the plasma deposition and growth of surface structures on the CFs. With this regard, the use of plasma etching and deposition techniques in combination with self-assembly strategies to attach functional groups on the surface of CFs is very promising. This approach has potential to tailor the surface properties and to functionalise CFs in unprecedented ways.

Finally, the additional cost of vacuum treatments may be compensated by the improved performance of the CFs and composites. With this regard, even though the implementation of a continuous vacuum process is unlikely at this stage, novel technical solutions should be sought to minimise the down time of batch-production facilities.

Funding statement

The research leading to these results has received funding from the European Union's Seventh Framework Program (FP7/2007-2013) under the agreement no GA604248.

Abbreviations and acronyms

BET: Brunauer–Emmett–Teller theory for surface area calculation

CF: carbon fibre

CD: corona discharge

d_{002}: interlayer spacing

DC: direct current

DBD: dielectric barrier discharge

DETA: dimethylenetriamine

EB: electron beam

FWHM: full width at half maximum

HOPG: highly ordered pyrolytic graphite

HR-TEM: high resolution transmission electron microscopy

I_D/I_G: intensity ratio

I_D: Intensity of disordered (turbostratic) peak

IFSS: interfacial shear strength

I_G: intensity of graphitic peak

I_T/I_G: intensity ratio

I_T: Intensity of turbostratic (disordered) peak

IR: infra-red

$L_{a//}$: crystallite dimensions in the parallel direction

L_{aT}: crystallite dimensions in the transverse direction

L_C: stacking thickness

LPP: low pressure plasma

MPP: mesophase pitch

MW: microwave

PAN: poly-acrylonitrile

PIII: plasma immersion ion implantation

RF: radio frequency

SEM: scanning electron microscopy

STM: scanning tunnelling microscopy

TEPA: tetraethylenepentamine

TETA: triethylenetetramine

TEM: transmission electron microscopy

T_g: glass transition temperature

TPD: temperature programmed desorption

UVO: ultra-violet oxidation

WAXD: wide angle x-ray diffraction

XPS: X-ray photoelectron spectroscopy

XRD: X- ray diffraction

Z: misorientation angle

γ^D_S: Surface energy, dispersive component

γ^P_S: Surface energy, polar component

γ_S: Surface energy

References

1. Hoecker F and Karger-Kocsis J. Surface energetics of carbon fibers and its effects on the mechanical performance of CF/EP composites. *J Appl Polym Sci*. 1996; 59: 139-153.
2. Tang LG and Karoos JL. A review of methods for improving the interfacial adhesion between carbon fiber and polymer matrix. *Polym Composite*. 1997; 18: 100-113.
3. Zielke U, Hüttinger KJ and Hoffman WP. Surface oxidized carbon fibers: II. Chemical modification. *Carbon*. 1996; 34: 999-1005.
4. Severini F, Formaro L, Pegoraro M and Posca L. Chemical modification of carbon fiber surfaces. *Carbon*. 2002; 40: 735-741.
5. Donnet JB and Guilpain G. Surface treatments and properties of carbon fibers. *Carbon*. 1989; 27: 749-757.
6. Solís-Fernández P, Paredes JI, Cosío A, Martínez-Alonso A and Tascón JMD. A comparison between physically and chemically driven etching in the oxidation of graphite surfaces. *J Colloid Interf Sci*. 2010; 344: 451-459.
7. Dai Z, Shi F, Zhang B, Li M and Zhang Z. Effect of sizing on carbon fiber surface properties and fibers/epoxy interfacial adhesion. *App Surf Sci*. 2011; 257: 6980-6985.
8. Ehlert GJ, Galan U and Sodano HA. Role of surface chemistry in adhesion between ZnO nanowires and carbon fibers in hybrid composites. *ACS Appl Mater Interfaces*. 2013; 5: 635-645.
9. Käppler I, Hund RD and Cherif C. Surface modification of carbon fibres using plasma technique. *AUTEX Res J*. 2014; 14: 34-38.
10. Tiwari S, Sharma M, Panier S, Mutel B, Mitschang P and Bijwe J. Influence of cold remote nitrogen oxygen plasma treatment on carbon fabric and its composites with specialty polymers. *J Mater Sci*. 2011; 46: 964-974.

11. Chen Z, Dai XJ, Lamb PR, et al. Coating and functionalization of carbon fibres using a three-step plasma treatment. *Plasma Process Polym*. 2013; 10: 1100-1109.
12. Pittman Jr CU, He GR, Wu B and Gardner SD. Chemical modification of carbon fiber surfaces by nitric acid oxidation followed by reaction with tetraethylenepentamine. *Carbon*. 1997; 35: 317-331.
13. Jones C and Sammann E. The effect of low power plasmas on carbon fibre surfaces: A comparison between low and high modulus PAN based fibres with pitch based carbon fibres. *Carbon*. 1990; 28: 515-519.
14. Yuan LY, Chen CS, Shyu SS and Lai JY. Plasma surface treatment on carbon fibers. Part 1: Morphology and surface analysis of plasma etched fibers. *Compos Sci Technol*. 1992; 45: 1-7.
15. Wu Z, Pittman Jr CU and Gardner SD. Nitric acid oxidation of carbon fibers and the effects of subsequent treatment in refluxing aqueous NaOH. *Carbon*. 1995; 33: 597-605.
16. Frank E, Steudle LM, Ingildeev D, Spörl JM and Buchmeiser MR. Carbon Fibers: Precursor Systems, Processing, Structure, and Properties. *Angew Chem Int Edit*. 2014; 53: 5262-5298.
17. Thunga M, Chen K, Grewell D and Kessler MR. Bio-renewable precursor fibers from lignin/polylactide blends for conversion to carbon fibers. *Carbon*. 2014; 68: 159-166.
18. Hughes JDH. The carbon fibre/epoxy interface—A review. *Compos Sci Technol*. 1991; 41: 13-45.
19. Sharma M, Gao S, Mäder E, Sharma H, Wei LY and Bijwe J. Carbon fiber surfaces and composite interphases. *Compos Sci Technol*. 2014; 102: 35-50.
20. Li R, Ye L and Mai Y-W. Application of plasma technologies in fibre-reinforced polymer composites: a review of recent developments. *Compos Part A-Appl S*. 1997; 28: 73-86.

21. Bai YJ, Wang CG, Lun N, Wang YX, Yu MJ and Zhu B. HRTEM microstructures of PAN precursor fibers. *Carbon*. 2006; 44: 1773-1778.

22. Ge H, Liu H, Chen J and Wang C. The microstructure of polyacrylonitrile-stabilized fibers. *J Appl Polym Sci*. 2009; 113: 2413-2417.

23. Watt W, Phillips LN and Johnson W. High strength, high modulus carbon fibers. *The Engineer*. 1966; 221: 815.

24. Davé V, Prasad A, Marand H and Glasser WG. Molecular organization of lignin during carbonization. *Polymer*. 1993; 34: 3144-3154.

25. Marshall P and Price J. Topography of carbon fibre surfaces. *Composites*. 1991; 22: 388-393.

26. Matsui J. Surface properties of carbon fibers. *Crit Rev Surf Chem*. 1990; 1: 71.

27. Johnson DJ. Structure-property relationships in carbon fibres. *J Phys D Appl Phys*. 1987; 20: 286-291.

28. Guigon M, Oberlin A and Desarmot G. Microtexture and structure of some high tensile strength, PAN-base carbon fibres. *Fibre Sci Technol*. 1984; 20: 55-72.

29. Guigon M, Oberlin A and Desarmot G. Microtexture and structure of some high-modulus, PAN-base carbon fibres. *Fibre Sci Technol*. 1984; 20: 177-198.

30. Kowbel W, Hippo E and Murdie N. Influence of graphitization environment of pan based carbon fibers on microstructure. *Carbon*. 1989; 27: 219-226.

31. Edie DD. The effect of processing on the structure and properties of carbon fibers. *Carbon*. 1998; 36: 345-362.

32. Qin X, Lu Y, Xiao H, Wen Y and Yu T. A comparison of the effect of graphitization on microstructures and properties of polyacrylonitrile and mesophase pitch-based carbon fibers. *Carbon*. 2012; 50: 4459-4469.

33. Johnson DJ, Tomizuka I and Watanabe O. The fine structure of lignin-based carbon fibres. *Carbon*. 1975; 13: 321-325.

34. Li D, Lu C, Wu G, et al. Heat-induced Internal Strain Relaxation and its Effect on the Microstructure of Polyacrylonitrile-based Carbon Fiber. *J Mater Sci Technol*. 2014.

35. Chatterjee S and Saito T. Lignin-Derived Advanced Carbon Materials. *ChemSusChem*. 2015; 8: 3941-3958.

36. Bacon R and Tang MM. Carbonization of cellulose fibers-II. Physical property study. *Carbon*. 1964; 2.

37. Ogale AA, Zhang M and Jin J. Recent advances in carbon fibers derived from biobased precursors. *J Appl Polym Sci*. 2016; 133.

38. Baker DA and Rials TG. Recent advances in low-cost carbon fiber manufacture from lignin. *J Appl Polym Sci*. 2013; 130: 713-728.

39. Diaz A, Guizar-Sicairos M, Poeppel A, Menzel A and Bunk O. Characterization of carbon fibers using X-ray phase nanotomography. *Carbon*. 2014; 67: 98-103.

40. Chatterjee S, Jones EB, Clingenpeel AC, et al. Conversion of lignin precursors to carbon fibers with nanoscale graphitic domains. *ACS Sustainable Chemistry and Engineering*. 2014; 2: 2002-2010.

41. Morent R, De Geyter N, Verschuren J, De Clerck K, Kiekens P and Leys C. Non-thermal plasma treatment of textiles. *Surf Coat Tech*. 2008; 202: 3427-3449.

42. Qian X, Chen L, Huang J, Wang W and Guan J. Effect of carbon fiber surface chemistry on the interfacial properties of carbon fibers/epoxy resin composites. *J Reinf Plast Comp*. 2013; 32: 393-401.

43. Nohara LB, Filho GP, Nohara EL, Kleinke MU and Rezende MC. Evaluation of carbon fiber surface treated by chemical and cold plasma processes. *Mat Res*. 2005; 8: 281-286.

44. Tiwari S and Bijwe J. Various ways to strengthen the fiber-matrix interface for enhanced composite performance. *Surf Interface Anal*. 2013; 45: 1838-1848.

45. Song W, Gu A, Liang G and Yuan L. Effect of the surface roughness on interfacial properties of carbon fibers reinforced epoxy resin composites. *App Surf Sci*. 2011; 257: 4069-4074.

46. Kafi A, Huson M, Creighton C, et al. Effect of surface functionality of PAN-based carbon fibres on the mechanical performance of carbon/epoxy composites. *Compos Sci Technol*. 2014; 94: 89-95.

47. He J, Huang Y, Meng L, Cao H and Gu H. Effects of chain lengths, molecular orientation, and functional groups of thiols adsorbed onto CF surface on interfaclal properties of CF/epoxy composites. *J Appl Polym Sci*. 2009; 112: 3380-3387.

48. Li Z, Wu S, Zhao Z and Xu L. Influence of surface properties on the interfacial adhesion in carbon fiber/epoxy composites. *Surf Interface Anal*. 2014; 46: 16-23.

49. Pamula E and Rouxhet PG. Bulk and surface chemical functionalities of type III PAN-based carbon fibres. *Carbon*. 2003; 41: 1905-1915.

50. Vautard F, Fioux P, Vidal L, et al. Influence of an oxidation of the carbon fiber surface by boiling nitric acid on the adhesion strength in carbon fiber-acrylate composites cured by electron beam. *Surf Interface Anal*. 2013; 45: 722-741.

51. Langston TA and Granata RD. Influence of nitric acid treatment time on the mechanical and surface properties of high-strength carbon fibers. *J Compos Mater*. 2014; 48: 259-276.

52. Meng LH, Chen ZW, Song XL, Liang YX, Huang YD and Jiang ZX. Influence of high temperature and pressure ammonia solution treatment on interfacial behavior of carbon fiber/epoxy resin composites. *J Appl Polym Sci*. 2009; 113: 3436-3441.

53. Servinis L, Henderson LC, Gengenbach TR, Kafi AA, Huson MG and Fox BL. Surface functionalization of unsized carbon fiber using nitrenes derived from organic azides. *Carbon*. 2013; 54: 378-388.

54. Meng L, Fan D, Huang Y, Jiang Z and Zhang C. Comparison studies of surface cleaning methods for PAN-based carbon fibers with acetone, supercritical acetone and subcritical alkali aqueous solutions. *App Surf Sci*. 2012; 261: 415-421.

55. Jones C and Sammann E. The effect of low power plasmas on carbon fibre surfaces. *Carbon*. 1990; 28: 509-514.

56. Montes-Morán MA, Martínez-Alonso A, Tascón JMD, Paiva MC and Bernardo CA. Effects of plasma oxidation on the surface and interfacial properties of carbon fibres/polycarbonate composites. *Carbon*. 2001; 39: 1057-1068.

57. Cioffi MOH, Voorwald HJC, Ambrogi V, Monetta T, Bellucci F and Nicolais L. Tensile strength of radio frequency cold plasma treated PET fibers - Part I: Influence of environment and treatment time. *J Mater Eng Perform*. 2002; 11: 659-666.

58. Lu C, Chen P, Yu Q, Ding Z, Lin Z and Li W. Interfacial adhesion of plasma-treated carbon fiber/ poly(phthalazinone ether sulfone ketone) composite. *J Appl Polym Sci*. 2007; 106: 1733-1741.

59. Mao L, Wang Y, Zang Z, Zhu S, Zhang H and Zhou H. Amino-functionalization of carbon fibers through electron-beam irradiation technique. *J Appl Polym Sci*. 2014; 131.

60. Yang R, Zhang L, Wang Y, et al. An anisotropic etching effect in the graphene basal plane. *Adv Mater*. 2010; 22: 4014-4019.

61. Montes-Morán MA and Young RJ. Raman spectroscopy study of HM carbon fibres: Effect of plasma treatment on the interfacial properties of single fibre/epoxy composites. Part I: Fibre characterisation. *Carbon*. 2002; 40: 845-855.

62. Akbar D and Güngör TE. Study of high radio frequency plasma discharge effects on carbon fiber using Raman spectroscopy. *Surf Coat Tech*. 2014; 240: 233-242.

63. Tang S and Choi HS. Comparison of low- and atmospheric-pressure radio frequency plasma treatments on the surface modification of poly(methyl methacrylate) plates. *J Phys Chem C*. 2008; 112: 4712-4718.

64. Jang J and Yang H. Effect of surface treatment on the performance improvement of carbon fiber/polybenzoxazine composites. *J Mater Sci*. 2000; 35: 2297-2303.

65. Tamargo-Martínez K, Villar-Rodil S, Martínez-Alonso A and Tascón JMD. Chemical and structural modifications of carbon nanofibers with different degrees of graphitic order following oxygen plasma treatments. *Mater Chem Phys*. 2013; 138: 615-622.

66. Oyama HT and Wightman JP. Surface characterization of PVP-sized and oxygen plasma-treated carbon fibers. *Surf Interface Anal*. 1998; 26: 39-55.

67. Santos AL, Botelho EC, Kostov KG, Nascente PAP and Da Silva LLG. Atmospheric plasma treatment of carbon fibers for enhancement of their adhesion properties. *IEEE T Plasma Sci*. 2013; 41: 319-324.

68. Xie J, Xin D, Cao H, et al. Improving carbon fiber adhesion to polyimide with atmospheric pressure plasma treatment. *Surf Coat Tech*. 2011; 206: 191-201.

69. Erden S, Ho KKC, Lamoriniere S, Lee AF, Yildiz H and Bismarck A. Continuous atmospheric plasma oxidation of carbon fibres: Influence on the fibre surface and bulk properties and adhesion to polyamide 12. *Plasma Chem Plasma Process*. 2010; 30: 471-487.

70. Jang BZ. Control of interfacial adhesion in continuous carbon and kevlar fiber reinforced polymer composites. *Compos Sci Technol*. 1992; 44: 333-349.

71. Sun Y, Liang Q, Chi H, et al. The application of gas plasma technologies in surface modification of aramid fiber. *Fiber Polym*. 2014; 15: 1-7.

72. Desimoni E, Salvi AM, Biader Ceipidor U and Casella IG. Activation of carbon fibres by negative d.c. corona discharge at ambient pressure and temperature. *J Electron Spectrosc*. 1994; 70: 1-9.

73. Da Silva LLG, Alves LG, Tóth A and Ueda M. A study of the effect of nitrogen and air plasma immersion ion implantation treatments on the properties of carbon fiber. *IEEE T Plasma Sci*. 2011; 39: 3067-3071.

74. von Engel A. *Ionized gases*. 2nd ed. Oxford: Clarendon Press, 1965, p.326.

75. Atkins PW. *Physical chemistry*. 3rd ed. Oxford: Oxford University Press, 1987, p.857.

76. Boudou JP, Paredes JI, Cuesta A, Martínez-Alonso A and Tascón JMD. Oxygen plasma modification of pitch-based isotropic carbon fibres. *Carbon*. 2003; 41: 41-56.

77. Cvelbar U. Interaction of non-equilibrium oxygen plasma with sintered graphite. *App Surf Sci*. 2013; 269: 33-36.

78. Sugai I, Oyaizu M, Takeda Y, Kawakami H, Hattori H and Kawasaki K. Influence of carbon material and sputtering angle on stripper foil lifetime. *Nucl Instrum Meth A*. 2010; 613: 448-452.

79. Sharma M, Bijwe J, Singh K and Mitschang P. Exploring potential of Micro-Raman spectroscopy for correlating graphitic distortion in carbon fibers with stresses in erosive wear studies of PEEK composites. *Wear*. 2011; 270: 791-799.

Figures

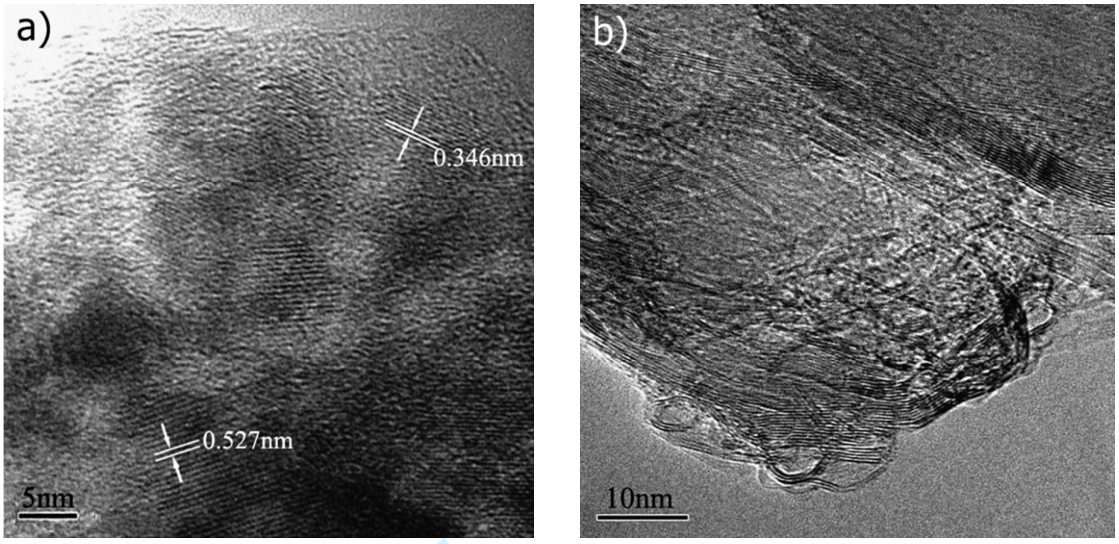

Figure 1: HR-TEM micrographs of PAN fibres: a) transverse and b) longitudinal cross-sections [21].

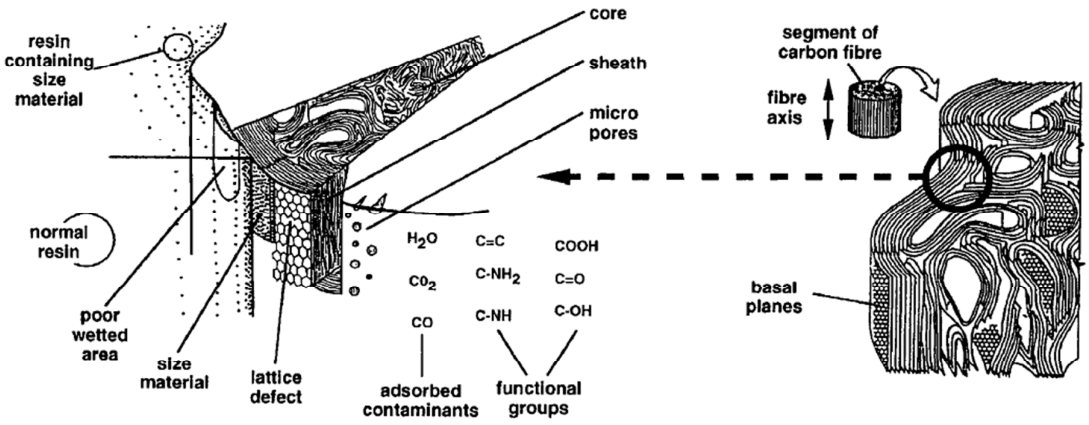

Figure 2: Schematic diagram of the surface structure of ex-PAN carbon fibres [1]

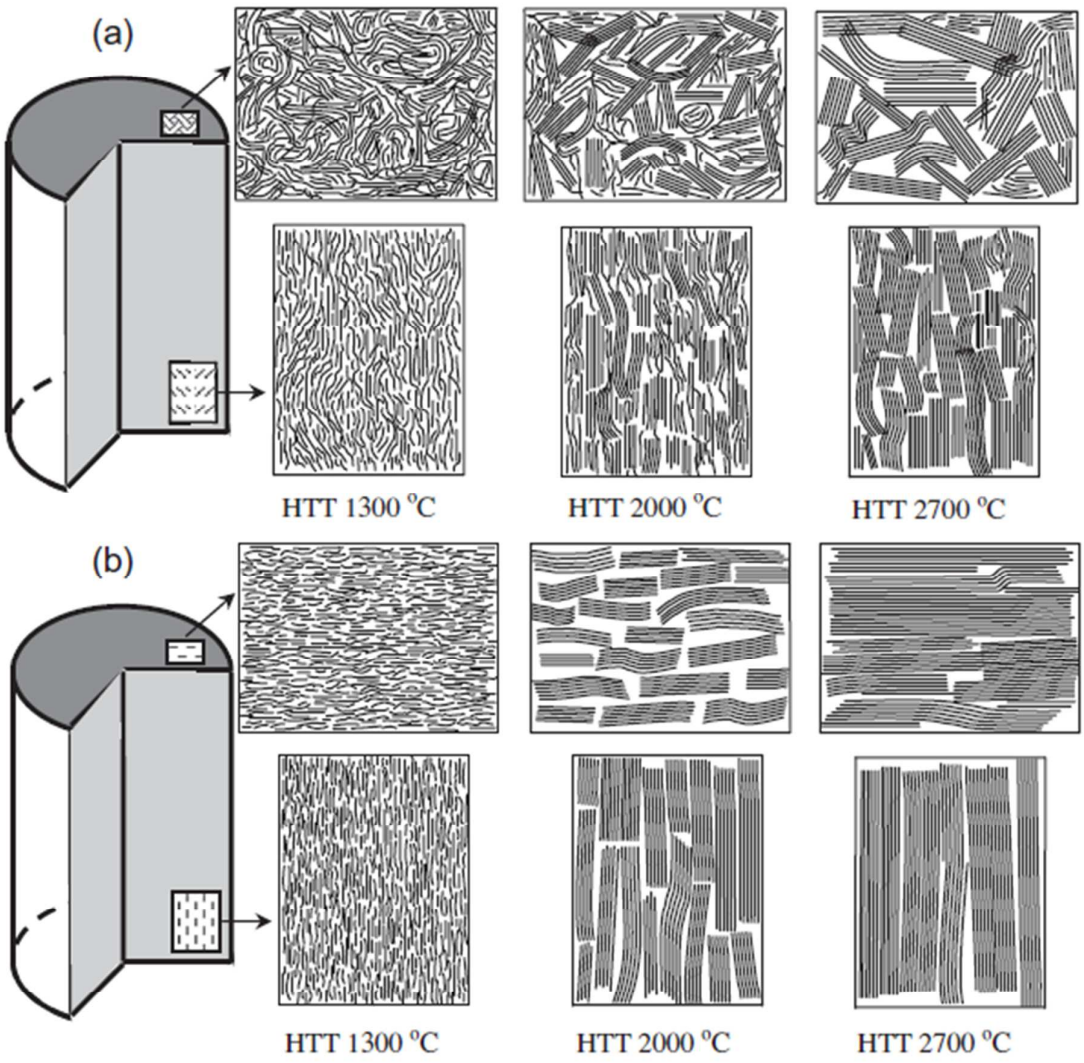

Figure 3: Proposed mechanism for the microstructural rearrangement and crystallite growth in the transverse and longitudinal sections of carbon fibres: a) ex-PAN and b) ex-MPP [32].

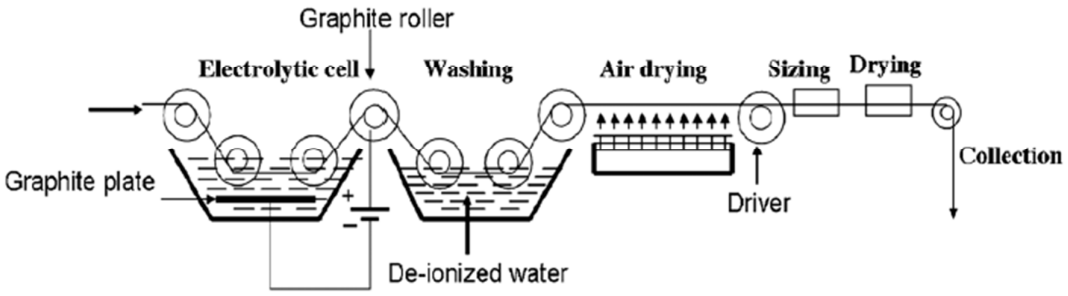

Figure 4: Schematic diagram of the equipment used in [48] for the surface functionalisation of carbon fibres by electrochemical oxidation.

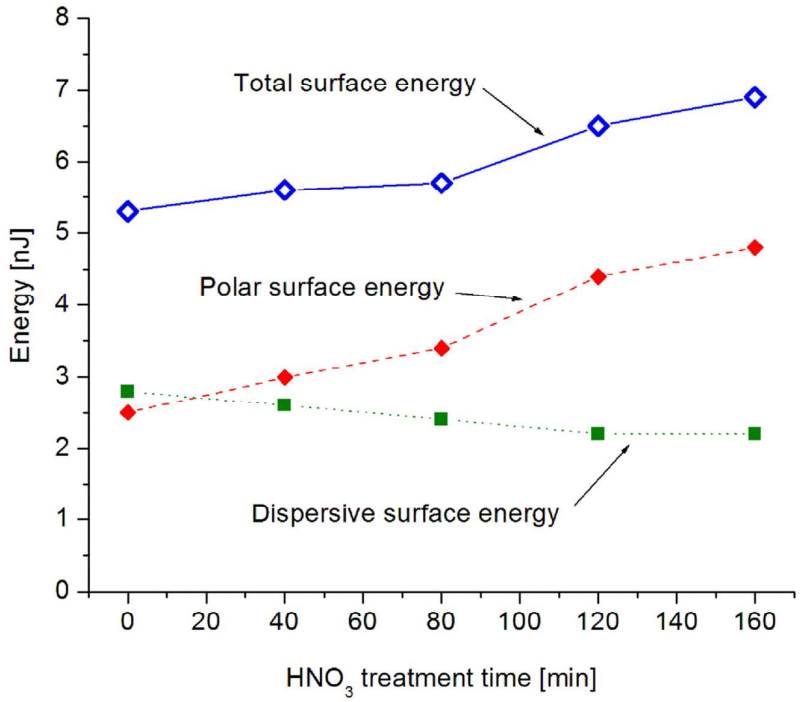

Figure 5: Surface energy of carbon fibres functionalised with nitric acid as a function of the treatment time [51].

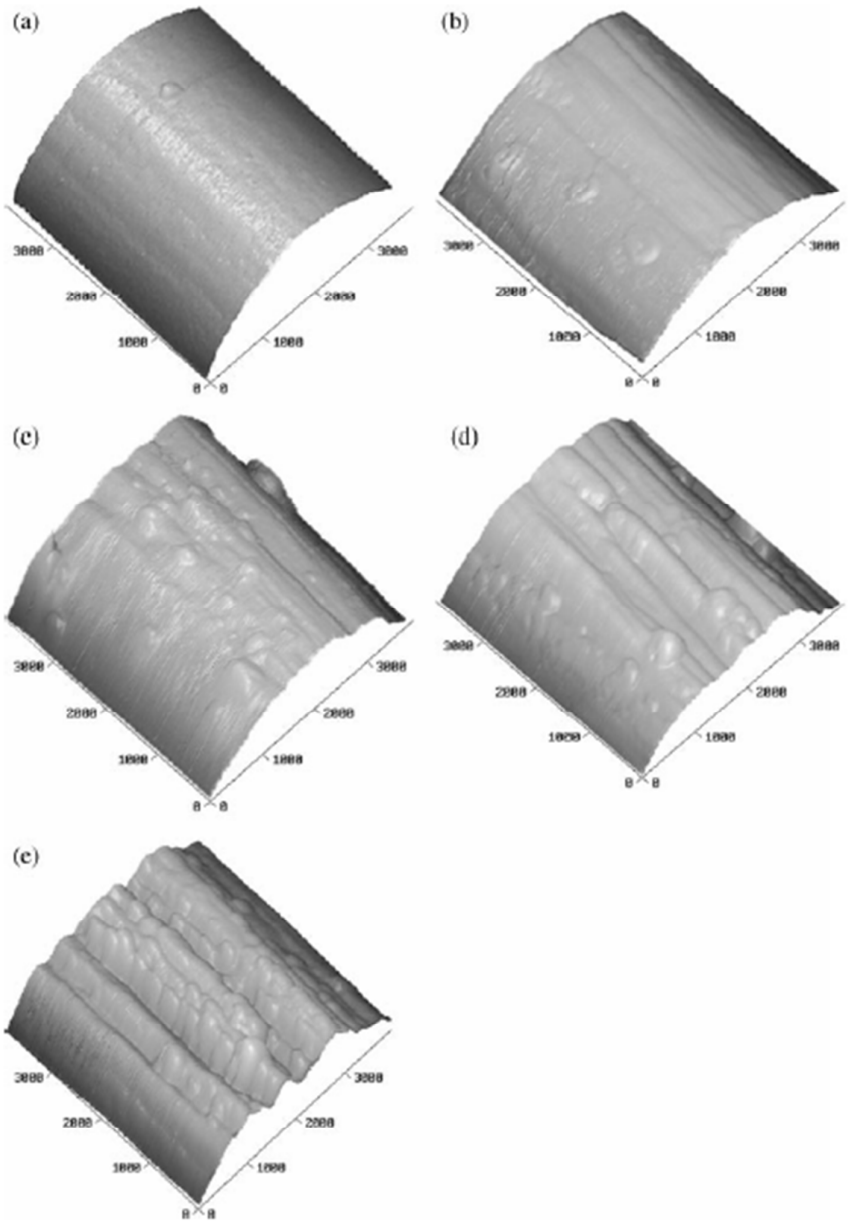

Figure 6: AFM surface profile of carbon fibres after plasma treatments with increasing time:

a) untreated, b) 5 c) 10 d) 15 and e) 20 minutes [58].

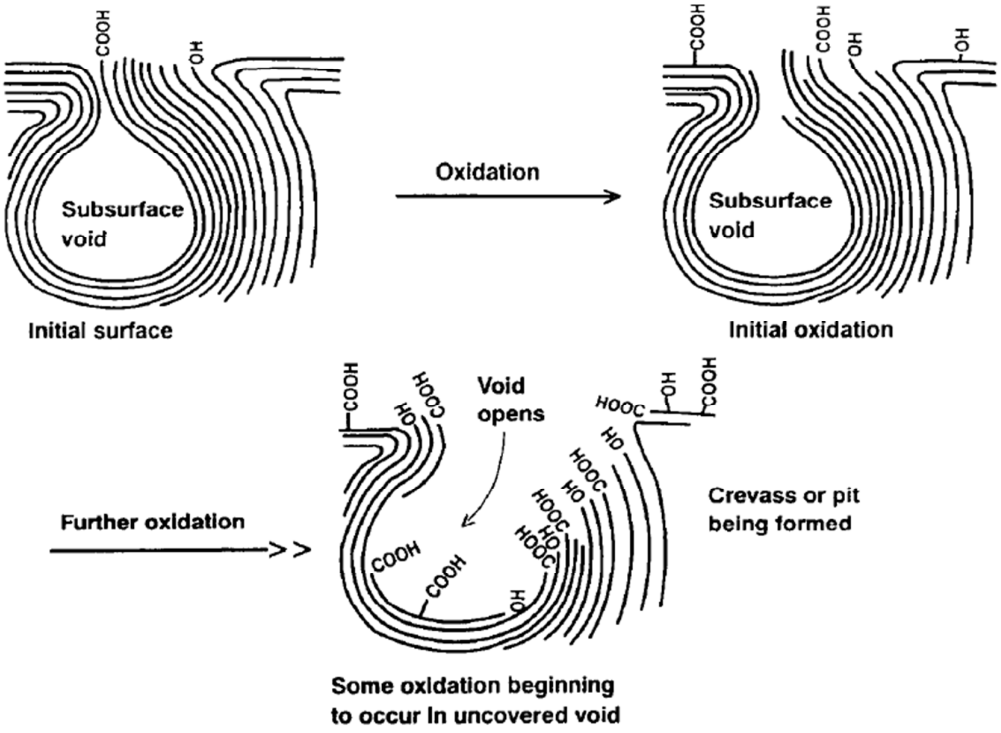

Figure 7: Proposed mechanism for the preferential oxidation which occurs at surface defects during functionalisation of carbon fibres with nitric acid [12].

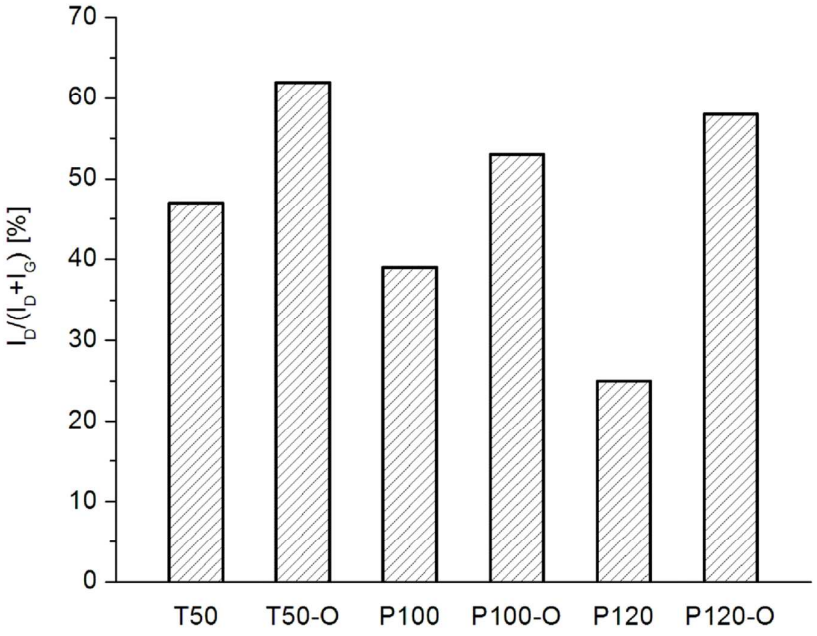

Figure 8: Structural order parameter $I_D/(I_D+I_G)$ of untreated and plasma oxidised (O) carbon fibres [61].

Note: T50 is an ex-MPP carbon fibre, while P100 and P120 are ex-PAN carbon fibres.

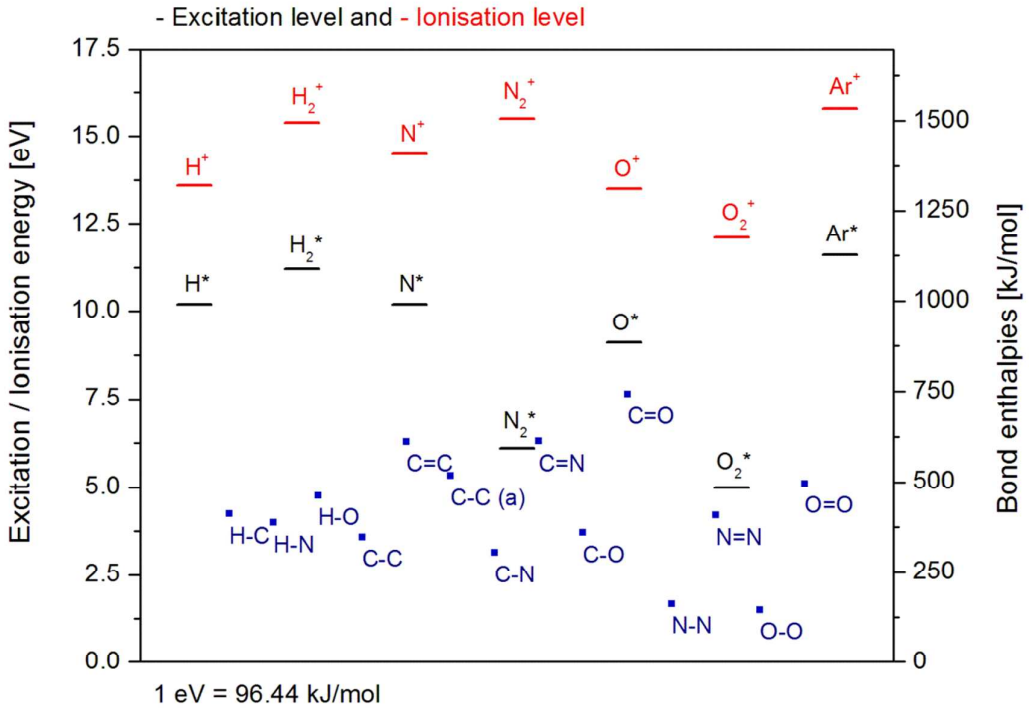

Figure 9: Illustration of the energy levels of active species in the plasma and the strength of chemical bonds found in carbon fibres. Data from [74, 75].

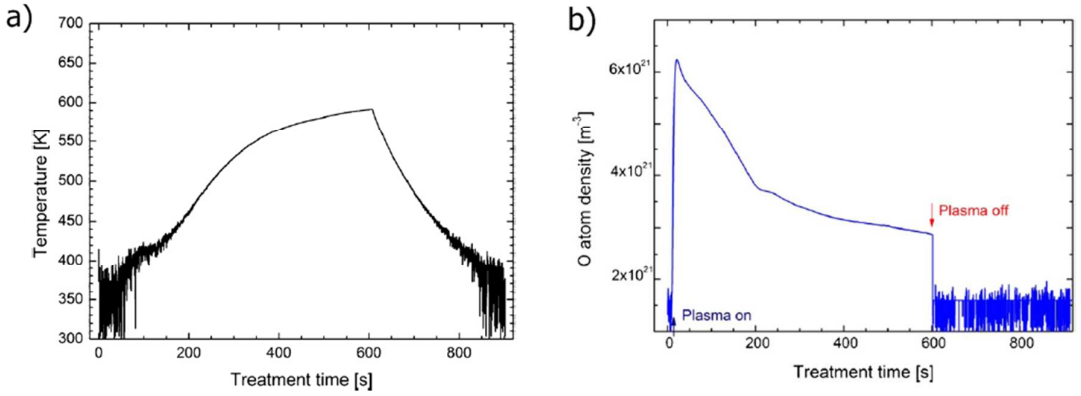

Figure 10: Parameters measured during the RF plasma treatment of sintered graphite: a) temperature of the substrate and b) concentration of oxygen atoms in the plasma [77].

Tables

Table 1: Crystalline dimensions obtained from HR-TEM images on ex-PAN and ex-MPP carbon fibres [32, 33]

Sample	d_{002} [nm]	$L_C^{\pm}$ [nm]		$L_{a//}$ [nm]	L_{aT} [nm]	Z [°]	$I_T/I_G^{\dagger}$
PAN 1300°C	0.3570	1.5	2.0	4.0	4.3	36.72	0.612
PAN 2000°C	0.3463	3.5	3.5	6.0	9.5	29.70	0.514
PAN 2500°C	0.3430	5.7	5.3	19	12	20.70	0.338
PAN 2700°C	0.3429	7.0	7.0	23	14	19.62	0.271
MPP 1300°C	0.3512	2.6	2.7	5.5	5.0	24.66	0.561
MPP 2000°C	0.3419	8	13	27	20	10.44	0.201
MPP 2500°C	0.3377	18	27	45	33	6.84	0.203
MPP 2700°C	0.3387	23	30	66	36	8.64	0.196
Lignin 1500°C	0.3450	1.0		2.0			
Lignin 2000°C	0.3430	2.1		4.0			

$^{\pm}$Transverse section and longitudinal section
†Results obtained from X-ray diffraction studies

Table 2: Typical properties of surface functionalised ex-PAN carbon fibres

Surface treatment	Functional groups	Filament strength*	Interlaminar shear strength*	Ref.
Electrochemical oxidation	C-OH, C=O, O-C=O	-15% to 0%	0% to +25%	42, 46, 48
Nitric oxidation	COOH, C=O, NH_x	-15% to +20%	+15% to +45%	15, 50, 51
Aqueous ammonia	COOH, C-NH_x	-20% to 0%	+5% to +50%	4, 45, 52
Atmospheric plasma	COOH, C=O	-15% to 0%	+40% to +70%	67-69
Low pressure plasma	COOH, C=O, NH_x	-12% to 0%	0% to +13%	56, 64, 70

* Relative to the untreated fibres; the range of values reflects different treatment conditions.

Table 3: Plasma technologies and surface interaction mechanisms

Method	Gas pressure	Effect on		IFSS mechanism	Ref
		Roughness	Filament strength		
Microwaves (MW)	Vacuum	↑	↓	Chemical	20, 56
Radio Frequency (RF)	Vacuum	↑↑	↓↓	Chemical-Physical	20, 64
Plasma immersion ion implantation	Vacuum	↑↑	↓↓	Chemical-Physical	73
Direct Current (DC)	Vacuum	↑↑↑	↓↓↓	Physical-Chemical	14, 20
Dielectric barrier discharge (DBD)	Atmospheric	↑↑↑↑	↓↓↓↓	Physical-Chemical	6, 67
Corona discharge (CD)	Atmospheric	↑↑↑↑↑	↓↓↓↓↓	Physical	20, 72

* The severity of the plasma treatment depends on the power level and the gas mixture

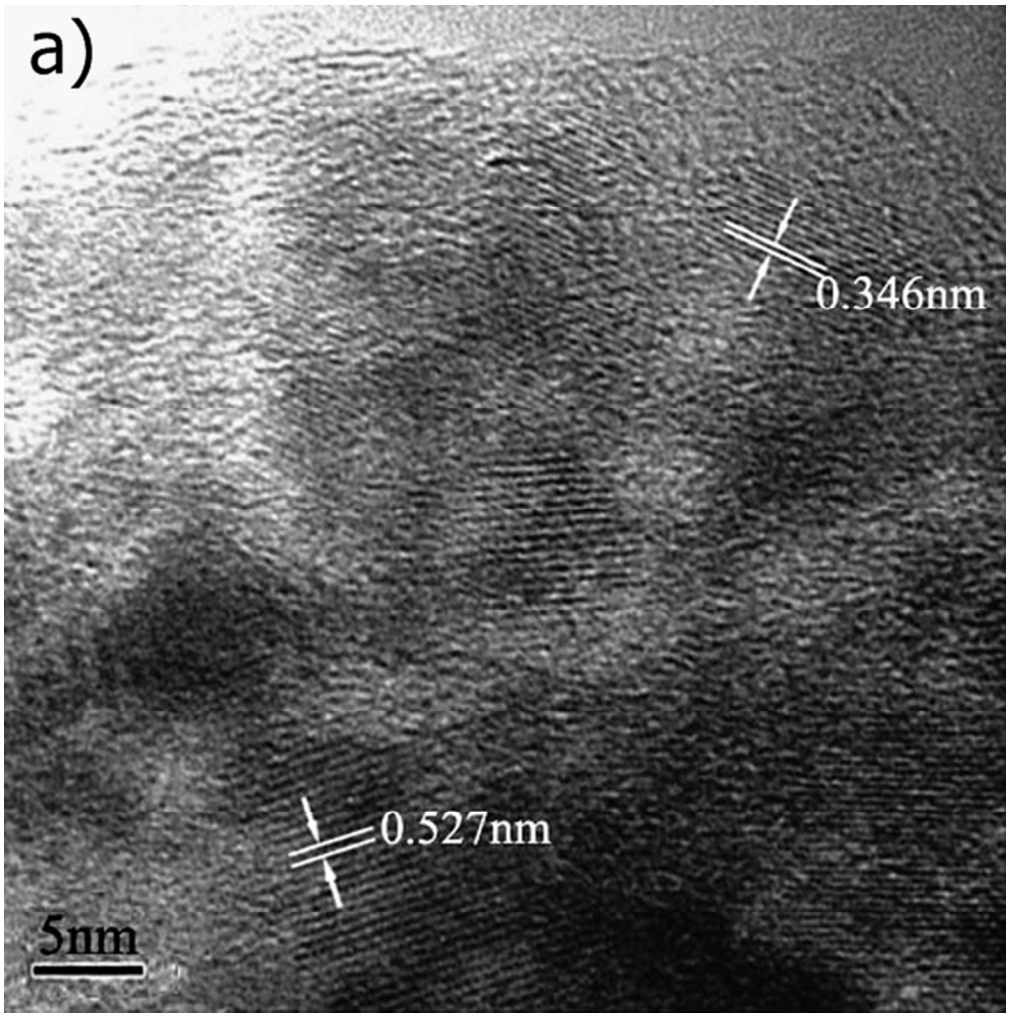

Figure 1a: HR-TEM micrographs of PAN fibres: transverse cross-section [21].

175x177mm (96 x 96 DPI)

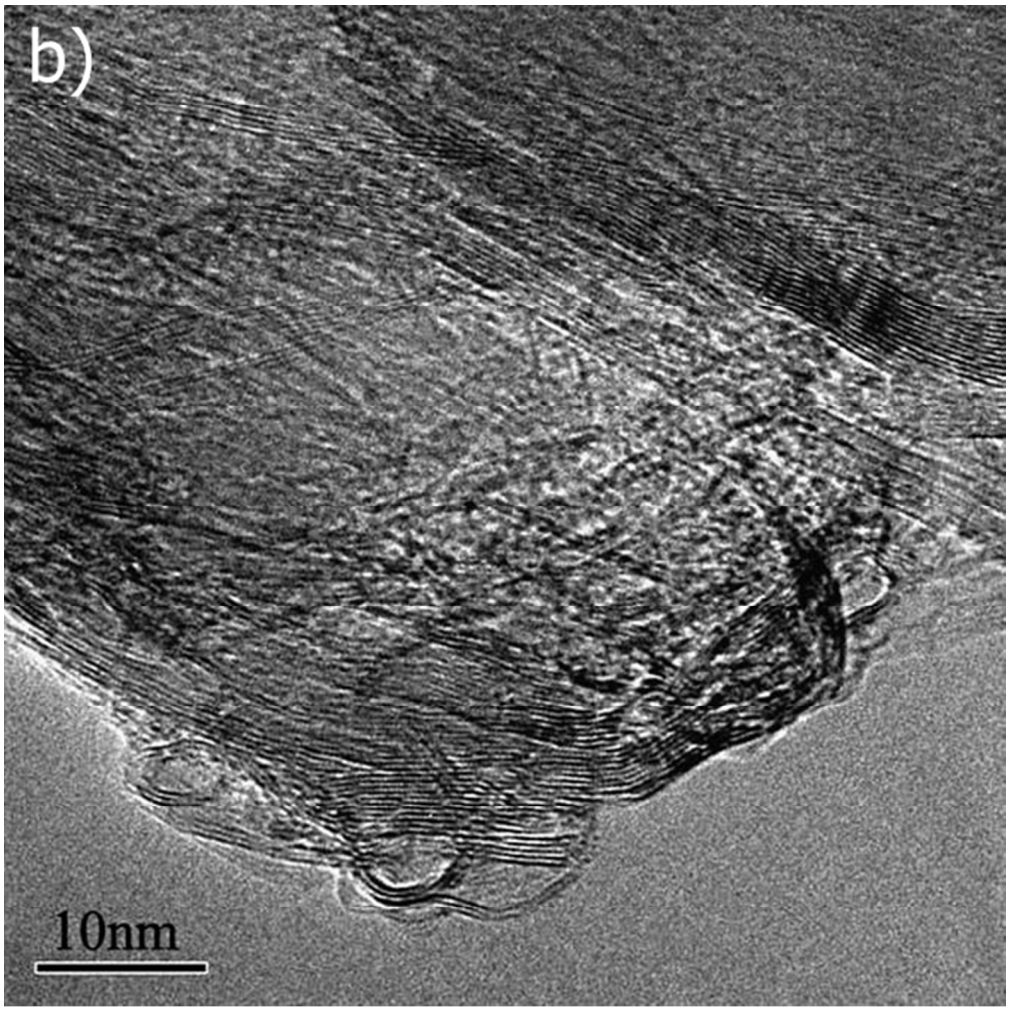

Figure 1b: HR-TEM micrographs of PAN fibres: longitudinal cross-section [21]

177x177mm (96 x 96 DPI)

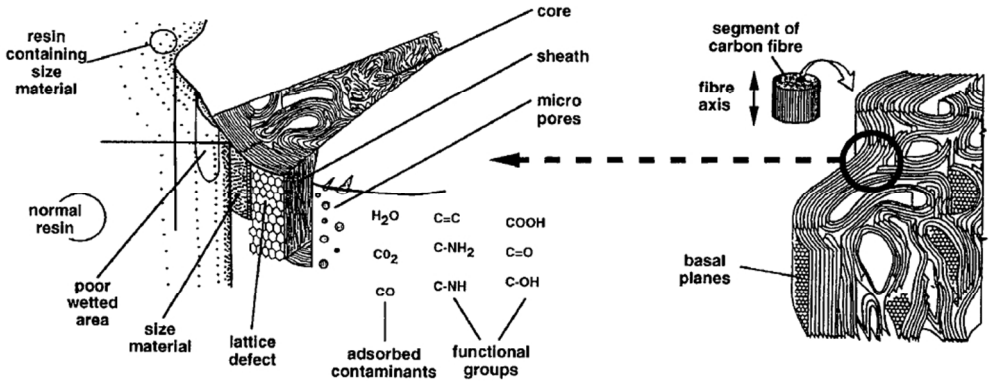

Figure 2: Schematic diagram of the surface structure of ex-PAN carbon fibres 25, 26 cited in 1.

278x111mm (96 x 96 DPI)

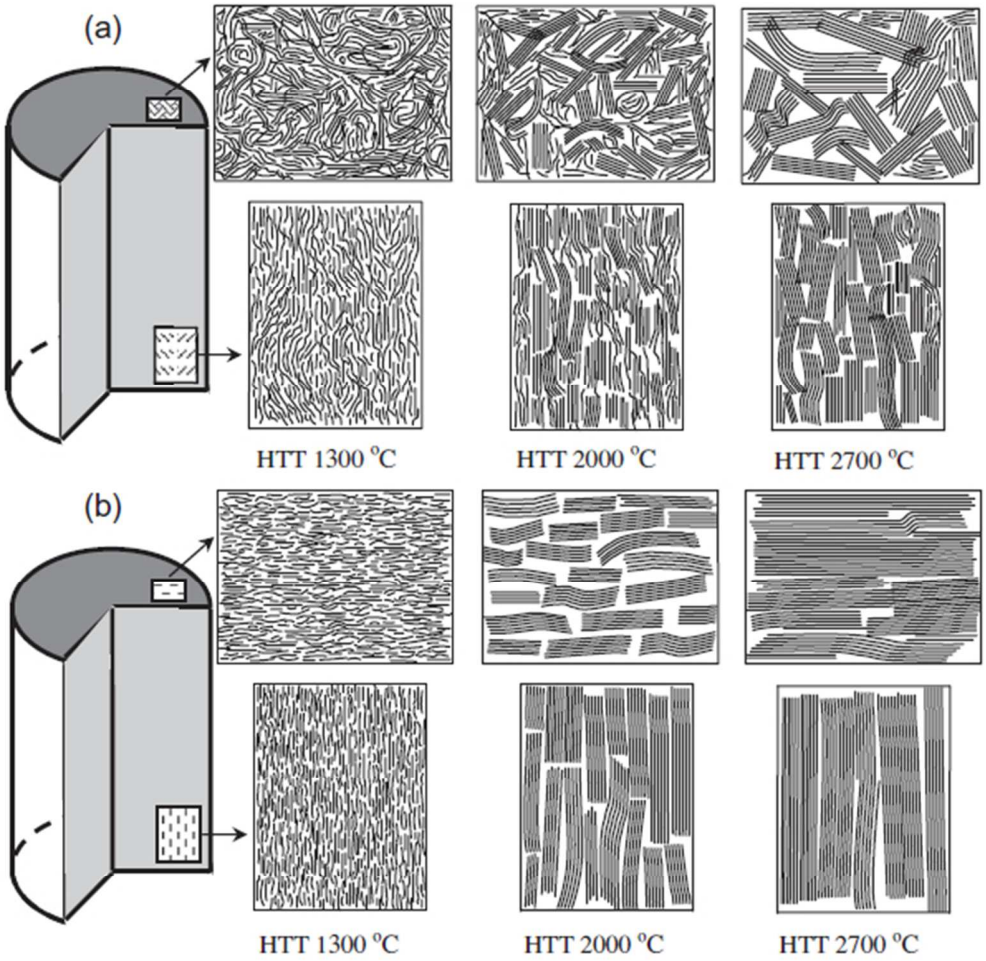

Figure 3: Proposed mechanism for the microstructural rearrangement and crystallite growth in the transverse and longitudinal sections of carbon fibres: a) ex-PAN and b) ex-MPP [25].

160x157mm (96 x 96 DPI)

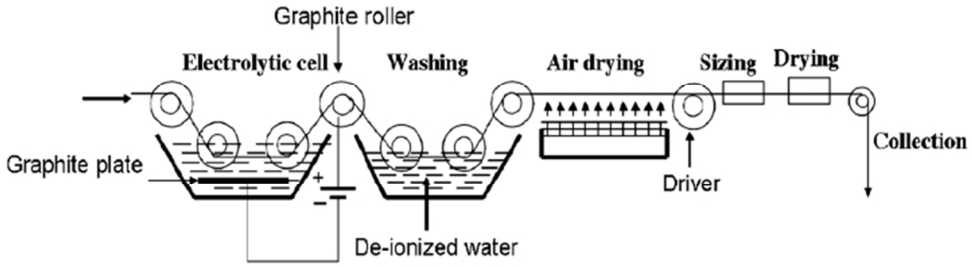

Figure 4: Schematic diagram of the equipment used in [61] for the surface functionalisation of carbon fibres by electrochemical oxidation

196x58mm (96 x 96 DPI)

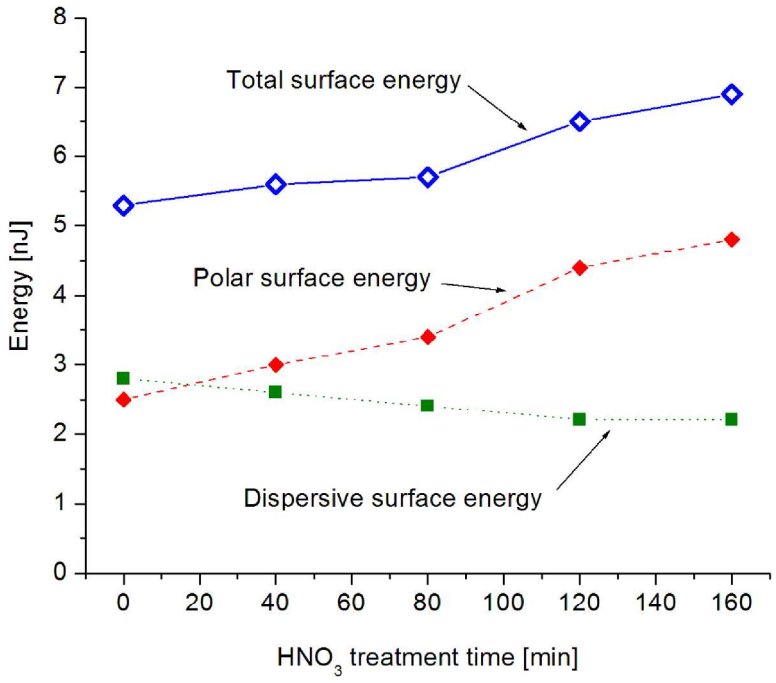

Figure 5: Surface energy of carbon fibres functionalised with nitric acid as a function of the treatment time
51.

279x215mm (200 x 200 DPI)

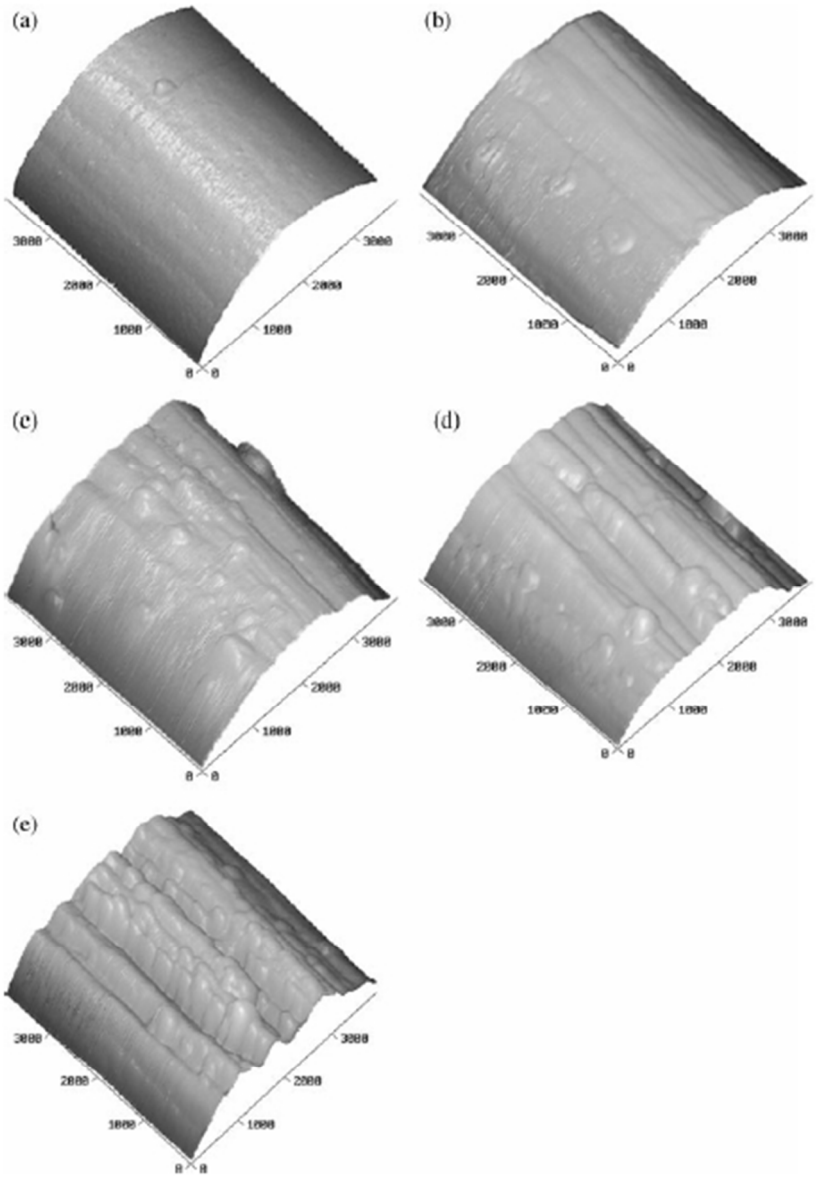

Figure 6: AFM surface profile of carbon fibres after plasma treatments with increasing time: a) untreated, b) 5 c) 10 d) 15 and e) 20 minutes 58.

120x168mm (96 x 96 DPI)

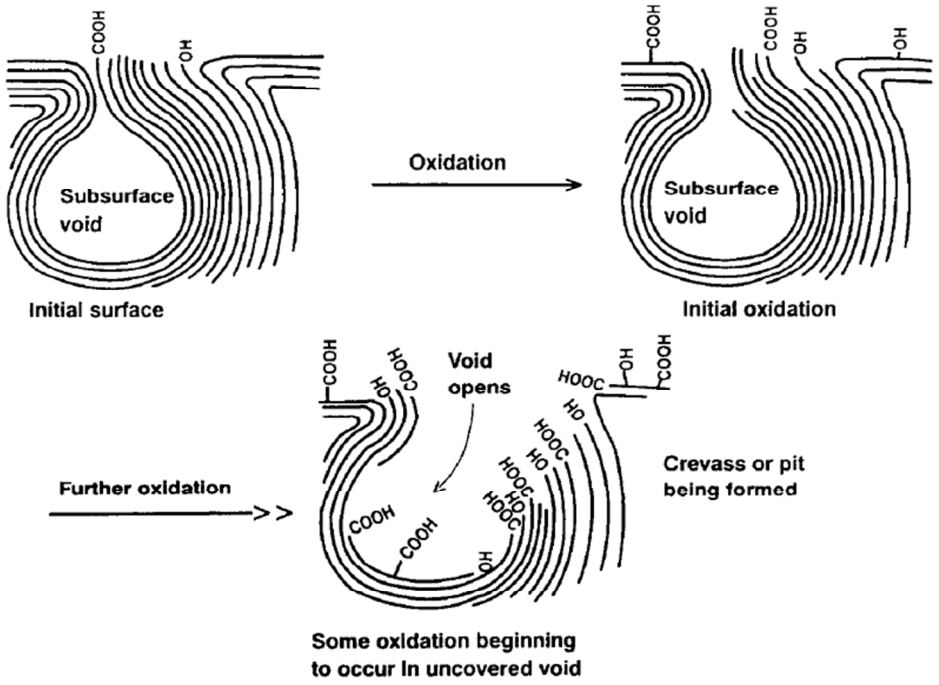

Figure 7: Proposed mechanism for the preferential oxidation which occurs at surface defects during functionalisation of carbon fibres with nitric acid 12.

225x158mm (96 x 96 DPI)

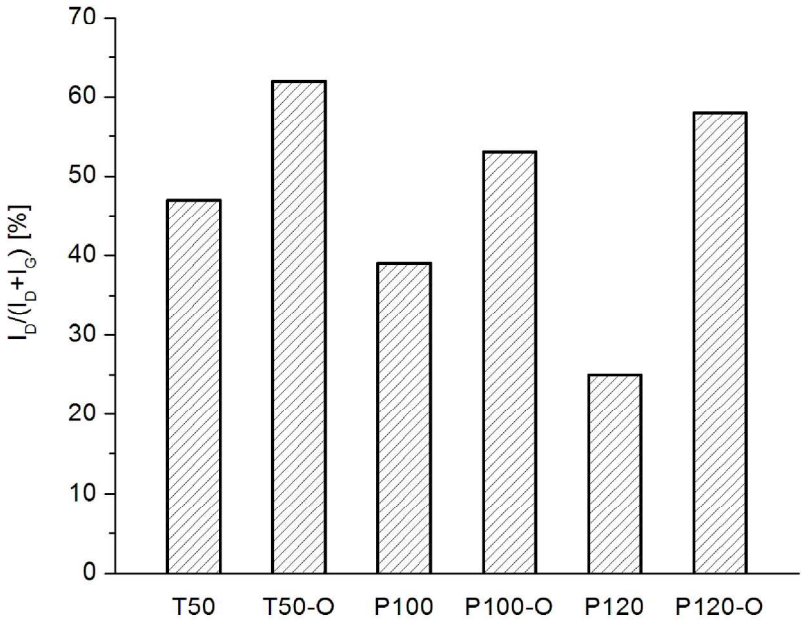

Figure 8: Structural order parameter ID/(ID+IG) of untreated and plasma oxidised (O) carbon fibres [46].
Note: T50 is an ex-MPP carbon fibre, while P100 and P120 are ex-PAN carbon fibres.

279x215mm (200 x 200 DPI)

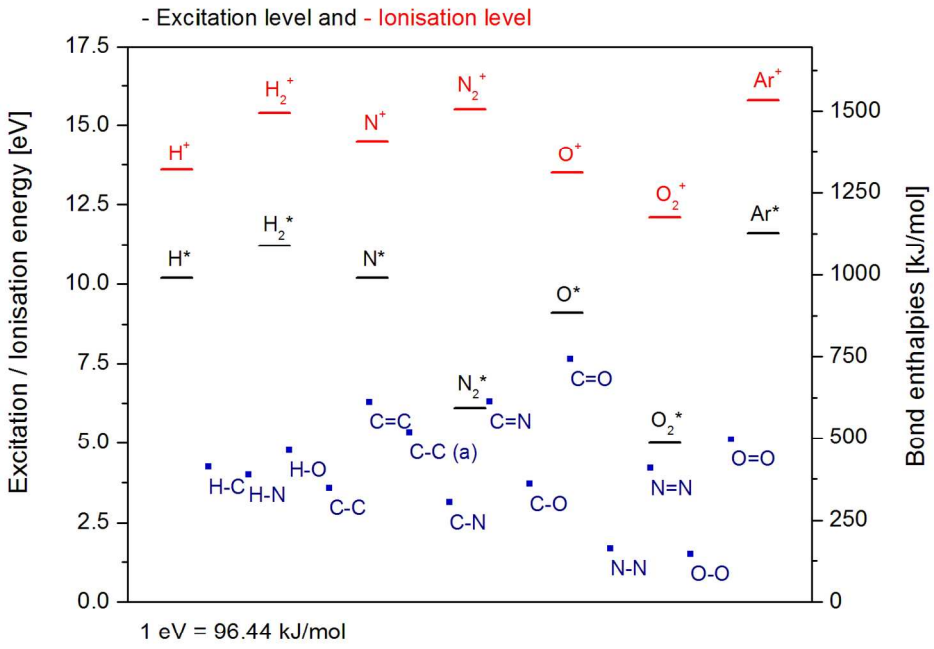

Figure 9: Illustration of the energy levels of active species in the plasma and the strength of chemical bonds found in carbon fibres. Data from 74, 75.

279x215mm (150 x 150 DPI)

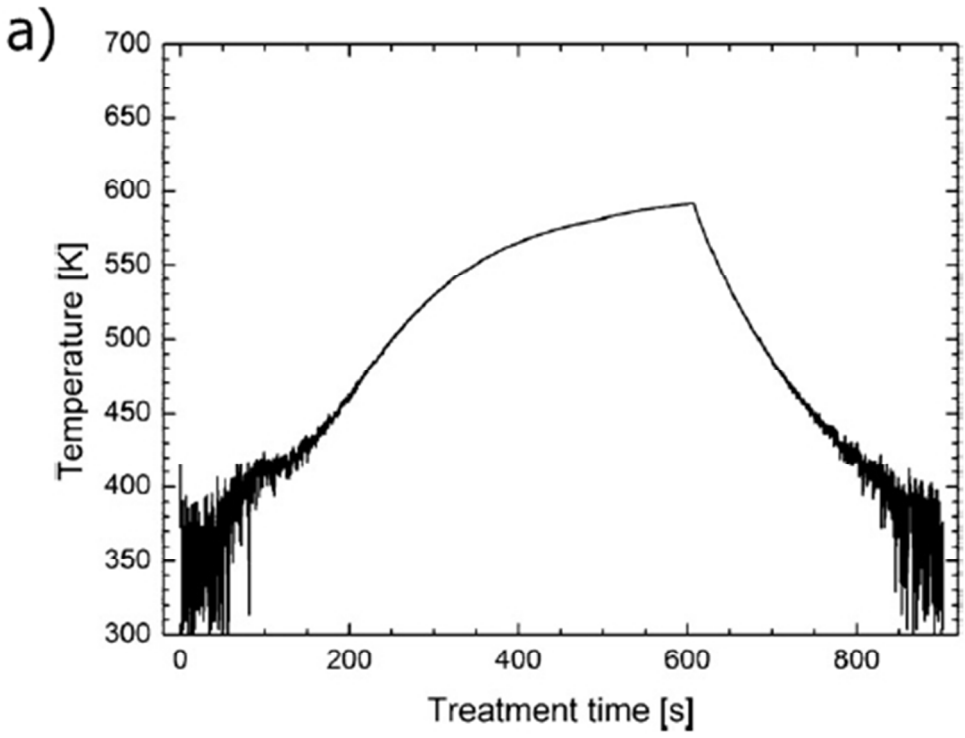

Figure 10: Parameters measured during the RF plasma treatment of sintered graphite: a) temperature of the substrate.

134x101mm (96 x 96 DPI)

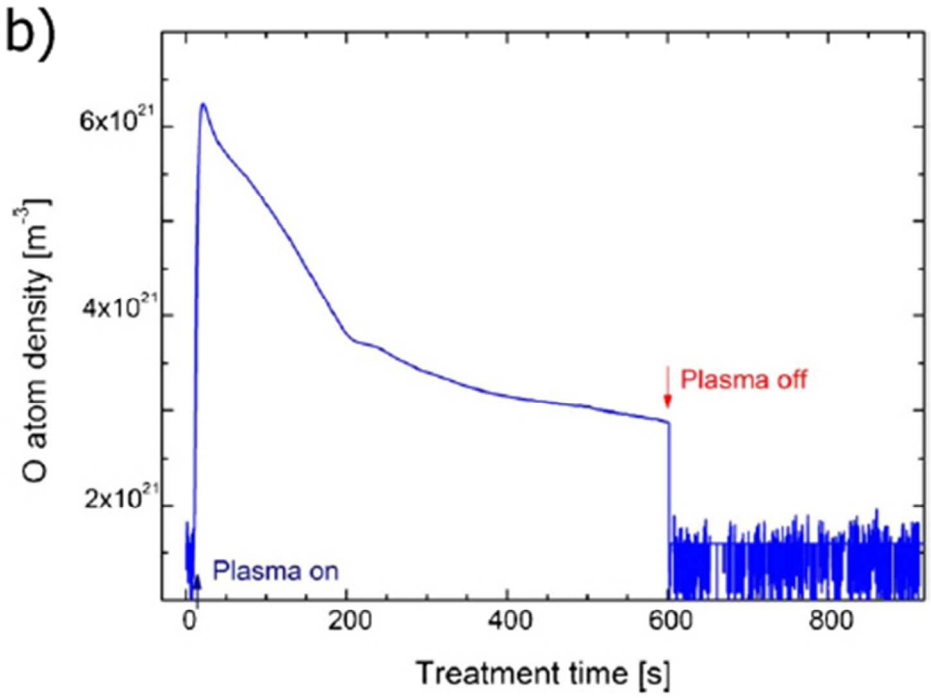

Figure 10: Parameters measured during the RF plasma treatment of sintered graphite: b) concentration of oxygen atoms in the plasma 77.

128x95mm (96 x 96 DPI)